CORA Cork Open Research Archive
Cartlann Taighde Oscailte Chorcaí

Title	Optical spectroscopy for biological and biomedical applications: potentially impacting future of healthcare with research, clinical translation and education
Authors	Saito Nogueira, Marcelo
Publication date	2021-11-10
Original Citation	Saito Nogueira, M. 2021. Optical spectroscopy for biological and biomedical applications: potentially impacting future of healthcare with research, clinical translation and education. PhD Thesis, University College Cork.
Type of publication	Doctoral thesis
Rights	© 2021, Marcelo Saito Nogueira. - https://creativecommons.org/licenses/by-nc-sa/4.0/
Download date	2026-11-16 11:57:31
Item downloaded from	https://hdl.handle.net/10468/14150

UCC
University College Cork, Ireland
Coláiste na hOllscoile Corcaigh

Chapter 8

Optical techniques

Marcelo Saito Nogueira

This chapter is part of the thesis "Optical spectroscopy for biological and biomedical applications: potentially impacting future of healthcare with research, clinical translation and education" by Marcelo Saito Nogueira

The rest of the thesis can be accessed via CORA UCC:

cora.ucc.ie

Please ensure appropriate acknowledgement and referencing when using material and/or ideas outlined in this thesis.

Contents

8. Optical techniques 289
8.1 Types of optical measurement techniques 290
8.1.1 Wavelength-resolved techniques 291
8.1.2 Spatially-resolved techniques 291
8.1.3 Spatial frequency-domain (SFD) techniques 292
8.1.4 Time-resolved (or time-domain) techniques 293
8.1.5 Frequency-domain (FD) techniques 296
8.1.6 Other techniques 297
8.2 Optical processes and related techniques 299
8.2.1 Diffuse reflectance spectroscopy 301
8.2.2 Elastic scattering spectroscopy 303
8.2.3 Infrared (IR) spectroscopy 304
8.2.4 Raman spectroscopy 306
8.2.5 Fluorescence spectroscopy (FS) 307
8.3 References 312

8. Optical techniques

Once the reader has reached this point of the thesis, you should have understood application-based features determining the optical properties of biological media, and optical instrument/device design factors involving combinations of source-detector geometries and specifications such as (1) optical components, (2) modeling, (3) applications, (4) probe and detector specifications, and (5) requirements to achieve the probed depth. Chapter 8 describes how to combine application-based features and previously discussed device-design factors to select the optimal optical-measurement techniques and photophysical processes for a given application. To give such description, chapter 8 explains the principles of (1) wavelength-resolved, (2) spatially-resolved, (3) time-resolved (or time-domain), and (4) frequency domain, and other techniques, as well as advantages and disadvantages of optical methods such as diffuse reflectance spectroscopy (DRS), Infrared (IR) spectroscopy, fluorescence spectroscopy (FS), and Raman spectroscopy (RS).

First, it is important to note that optical techniques can be categorized by using multiple types of classification including:

- Optical measurement techniques consisting of ways to perform optical measurements based on the available instrumentation, including aspects of illumination and light collection/detection. Examples include wavelength-resolved, spatially-resolved, time-resolved, spatial frequency-domain (SFD), frequency-domain (FD), polarization-resolved, and angular-resolved techniques as well as optical coherence tomography, laser-Doppler flowmetry and others.
- Imaging techniques, which involve multiple ways of being acquired and processed, given the recent advances in imaging instrumentation (which opened opportunities to multiple types of tomography, beam shaping, structured light imaging and single fiber imaging) and computational imaging (which enables research towards lens-free imaging, super-resolution imaging via machine learning methods without super-resolved microscopy techniques, etc).
- non-linear optical techniques such as second harmonic generation, multiphoton absorption, and stimulated emission techniques.
- Optical (photophysical) process techniques, which comprise of determining quantities associated with sample properties and specific photophysical processes such as absorption, elastic scattering, fluorescence, phosphorescence and Raman scattering.
- Optical (photochemical) process techniques, which consist of collecting data based on chemical processes induced by light such as absorption or luminescence lifetimes of metal–ligand complexes (e.g., ruthenium(II) complexes for oxygen sensing in, for example, photodynamic therapy studies), multiple optical processes arising from organic probes, polymer probes, nanoparticle probes [1].
- Photophysical process enhancement techniques such as UV resonance Raman spectroscopy (RRS), surface enhanced Raman scattering (SERS), coherent anti-Stokes Raman scattering (CARS) and stimulated Raman scattering (SRS) [2].
- Light penetration enhancement techniques such as optical clearing (deeper light penetration by refractive index matching upon application of external agents), wavefront shaping (focusing deeper into scattering media by optimization of incoming light beam based on transmission matrices), as well as techniques combining light and sound including acousto-optical tomography/imaging (collection of deeper photons by tagging frequency-shifted light due to the interaction between the laser beam and ultrasound at the ultrasound focus) and photoacoustics (detection of sound waves generated by absorption of light)
- Optical treatment techniques such as phototherapy, photothermal therapy, photodynamic therapy, sono-photodynamic therapy and others,

and that chapter 8 covers only optical-measurement and photophysical-process techniques.

8.1 Types of optical measurement techniques

In this section, we aim to show the types of optical measurement techniques available to date.

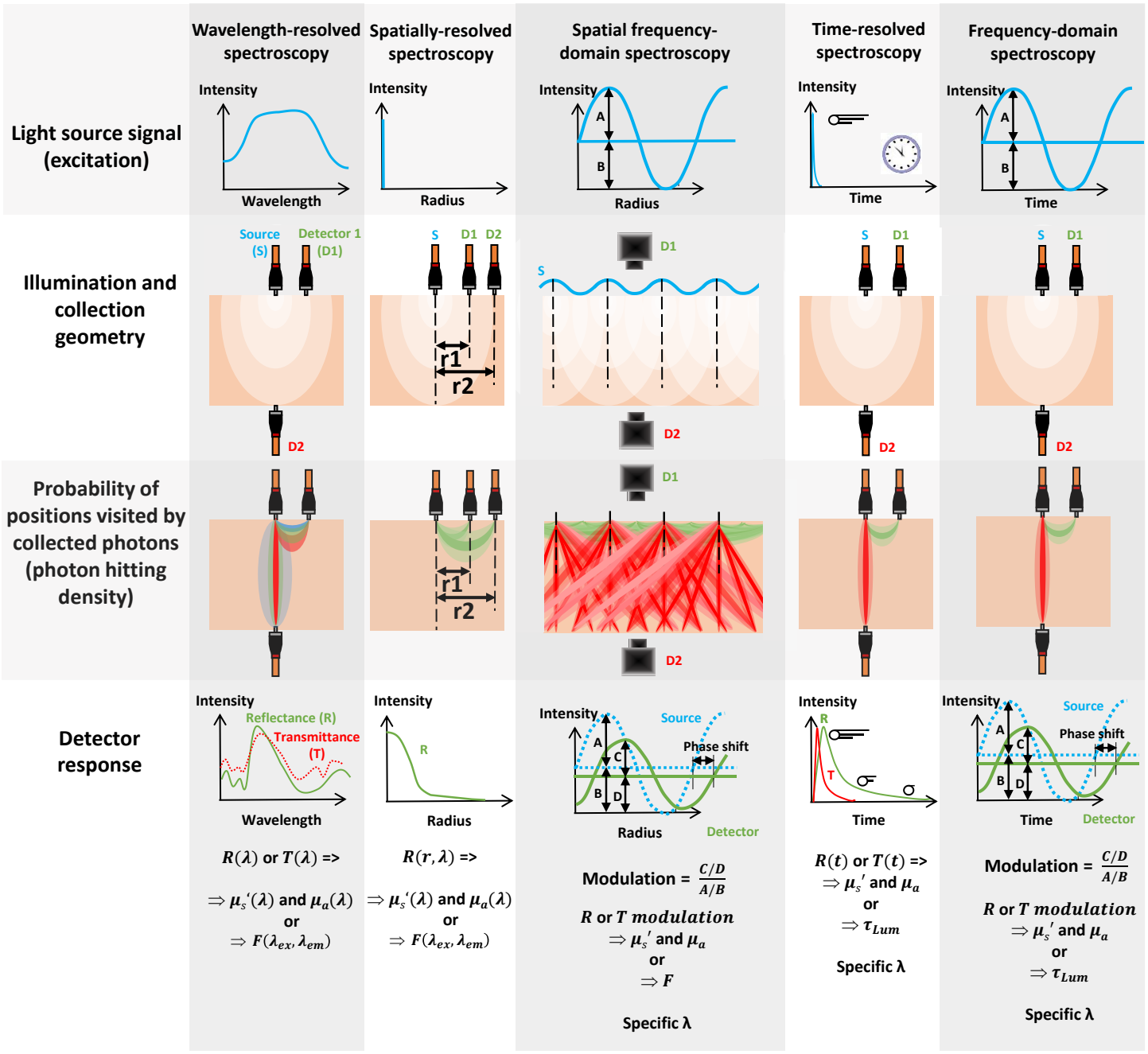


Figure 8.1: Schematic drawing of characteristics of optical measurement techniques (columns), including wavelength-resolved, spatially-resolved, spatial frequency-domain, time-resolved, and frequency-domain spectroscopy techniques. For each of these techniques, rows show characteristics such as the (1) light intensity as a function of the parameter varied at each technique, (2) spatial light distribution based on the source and detector positions, and the illumination profile, (3) the photon hitting density (PHD) based on the convolution of source and detector responses, and (4) the detector intensity-based measurements as a function of the pertinent variable corresponding to each optical measurement technique. Since spatial frequency-domain spectroscopy is based on spatially-modulated illumination at several positions (spatial periodically-varying intensity) and typically on light collection with imaging detectors (e.g., camera), the PHD is shown for several combinations of illumination and collection positions, assuming PHD is higher at positions of higher illumination intensity and detection to be uniform over the field of view of the imaging detector.

8.1.1 Wavelength-resolved techniques

The aim of wavelength-resolved techniques is determining tissue microstructural and biochemical information as well as biofluid composition based on the shape of wavelength-dependent spectra collected in reflectance or transmittance geometry (i.e., with source and detector fibers on the same surface or on opposite surfaces, respectively; figure 8.1). Obtaining this information is only possible because light penetrates into tissue and accumulates information on the tissue constitution due to the sequence of events it experiences while diffusing within it (chapter 4. Light-tissue interactions and light propagation in biological media). Tissue microstructure is associated with the particle distribution (which define how light travels/scatter into tissue; chapters 4 and 7, sections 4.5 and 7.1) in tissues and biofluids, whereas tissue biochemistry and biofluid constitution is associated with biomolecules which either only absorb or absorb and emit light differently as a function of wavelength (discussed in more detail in chapters 4 and 7, sections 4.2 and 7.3). Optical data is typically collected in continuous wave mode (i.e., with light sources continuously sending light to the sample and detectors continuously measuring the collected light) by sending light to tissue over a wide wavelength range and collecting the reflected or transmitted light (figure 8.1) with spectrometers which can be portable and, in most cases (currently), measuring the wavelength ranges within 200-3000 nm for tissues and within 300-25000 nm (50000–400 cm^{-1}). Wavelength-dependent quantities can also be expressed in terms of energy (typically in eV) and wavenumbers (typically cm^{-1} in near-infrared and mid-infrared spectroscopy). Tissue and biofluid responses as a function of wavelength are highly dependent on the illumination/collection geometry (chapter 6, section 6.2), and the tissue optical properties (chapter 4, section 4.1, and chapter 7), which describe the optical processes occurring into tissue (e.g., light scattering, absorption, fluorescence, phosphorescence, Raman scattering; chapter 4, figures 4.1 and 4.2). The types of biomolecules quantified with wavelength-resolved techniques are determined by the type of optical processes being considered (chapter 7). Analysis of wavelength-resolved signals is typically performed with machine learning methods or fitting the measured quantities (reflectance, transmittance, intensity of fluorescence and Raman scattered light) based on optical properties (anisotropy factor, scattering coefficients, absorption coefficients, fluorescence and/or Raman emission, chapter 4, section 4.1) of tissue constituents (chapter 7). The accuracy of microstructural and biochemical parameters obtained in the spectral fitting approach may be limited by the tissue heterogeneity due to the investigation of different probed depths at each wavelength, as these depths are dependent on optical properties which vary as a function of wavelength.

8.1.2 Spatially-resolved techniques

Spatially-resolved optical techniques are focused on monitoring the quantity of diffusely (and typically continuously) reflected or reemitted light as a function of the distance from the center of the incident beam (e.g.; r1 and r2; figure 8.1), which can be either normal or oblique to the tissue surface. As for non-hybrid wavelength-resolved techniques, spatially-resolved data is typically collected in continuous wave (CW) mode. The shape of the radial reflectance spectra is determined by optical properties which allow the determination of tissue microstructure and biochemistry (similarly to wavelength-resolved techniques). For instance, tissues with higher concentration of a certain absorbing molecule (chromophore) would lead to larger light intensity attenuation (quicker decay) as a function of the distance (radius) from the incident beam (chapter 5, section 5.2 Absorption processes). Reflectance data can be obtained even for larger distances between source and detector fibers (Figure 8.1), which typically range between 0 cm (illumination and collection with the same fiber) and 5 cm. Larger distances are typically found in brain tissue applications in the near-infrared wavelength range and other applications requiring larger tissue probed depth (chapter 6, section 6.5 Photon hitting density). The spatially-resolved data is usually analyzed by fitting the measured signal (reflectance, fluorescence intensity, Raman intensity) for tissue/biofluid/biosolid optical properties. This analysis allows obtaining information on sample biochemistry and microstructure. Spatially-resolved optical techniques may be limited by tissue heterogeneity due to the strong dependence of signals in reflectance geometry (i.e., with source and detector fibers on the same tissue surface) on the probed depth, which increases radially as a function of the distance from the incident beam.

8.1.3 Spatial frequency-domain (SFD) techniques

Similar to spatially-resolved optical techniques, the SFD counterparts monitor the intensity of reflected or reemitted light upon normal or oblique illumination of the tissue surface to extract tissue/biofluid/biosolid optical properties (and determine sample biochemistry and microstructure). However, SFD techniques:

- use illumination is based on structured light patterns of fixed spatial frequencies and phases (e.g., a sinusoidal pattern of light spatially projected on the sample surface).
- the data analysis requiring the signal amplitude modulation for determination of sample optical properties and other variables are based on demodulation techniques including:
    - single-pixel demodulation, where data is acquired from a single point/pixel over several times/frames with different phase shifts. Acquiring several frames increases the acquisition time and is suitable for applications where samples are stable over time and measurement time is not a limitation. Single-pixel demodulation is suitable for spatially inhomogeneous samples whose signal variation over time is much smaller than the measurement acquisition time.
    - multipixel demodulation (only applied to SFD imaging, also known as SFDI), which is based on the Fourier transform of a line of pixels or of the entire image. This demodulation is suitable for samples which are spatially homogeneous and can be used for accurate temporal measurements when the measurement acquisition time is smaller than the signal variation over time (more easily achievable upon acquisition of 1 point measurement or image frame).
- are typically combined with surface profilometry in the same instrumentation, as both are based on the projection of patterns of light on the sample surface. Surface profilometry is used to correct for signal acquisition at different angles and distances from the sample, which are necessary when the sample surface is inhomogeneous or when imaging at wide field of view (FoV). Combination with profilometry can enable 3-D surface measurements with corrected sample optical properties [3]. Currently, 3-D correction of sample optical properties can be made up to up to 75 degrees surface angle [4–6].
- are usually used for imaging and non-contact measurements (chapter 6, sections 6.1.1 and 6.2) while instrumentation can still be compact for integration of spatial frequency-domain imaging into endoscopes for extraction of tissue optical properties.
- demodulation requires additional calibration, as knowledge about the contribution of the optical system to the measured diffuse reflectance (and amplitude modulation) is necessary for data analysis.
- may be incorporated in more expensive instruments compared to those using spatially-resolved techniques, since such instruments usually require more sophisticated optical equipment and analysis.

The probed depth of SFD techniques depends on the spatial frequency used. Lower spatial frequencies lead to larger probed depth (similar to larger SDDs for spatially-resolved techniques; section 8.1.2 Spatially-resolved techniques and section 6.5 Photon hitting density). When using lower spatial frequencies intrinsic limitations of lower signal-to-noise ratio (SNR) are applicable in a similar way that SNR is decreased when using larger SDDs (sections 6.1.4 and 6.4.4 Larger or smaller spatial separation between light source and detector (i.e., larger or smaller source-to-detector distances; SDD)). Since most SFD measurements are non-contact and imaging, SNR can decrease even further due to the limitation of illumination power compared to point measurements (to keep compliance with laser safety requirements and prevent tissue heating). With this in mind, accuracy of determination of sample optical properties may decrease for lower spatial frequencies and non-contact imaging measurements.

It is worth noting that SFD techniques can be used for point spectroscopy when point detectors are used instead of cameras or scanning systems. Also, contact measurements are possible considering a subcase of spatially-resolved techniques for discrete structured light patterns by using sequences of optical fibers to illuminate sample surface at periodically-repeated space coordinates (e.g., figure 8.1 with r2 = 2 * r1 or with patterns of fibers placed at equal distances

from their adjacent illumination counterparts). More details about demodulation and analysis of SFD imaging signals can be found in the review by Gioux et al. [7]

In general, the analysis of spatially-resolved signals and point spectroscopy could be made via Fourier transform of the input light into a broad spectrum of sinusoidal components. Information of light propagation of spatially modulated signals over a broad frequency range could be performed by analyzing the distribution of one or more light sources of finite size in a similar way light propagation can be derived from time-resolved signals after predicting the light distribution of one temporal pulse of light via frequency modulated signals obtained from the Fourier transform of such pulse [8] (sections 8.1.4 Time-resolved (or time-domain) techniques and 8.1.5 Frequency domain techniques of this chapter).

8.1.4 Time-resolved (or time-domain) techniques

The concept of time-resolved techniques is registering the number of photons arriving at a certain tissue position in either reflectance or transmittance geometry (figure 8.1). In order to evaluate tissue absorption and scattering properties, or fluorescence/phosphorescence decay signals, instruments conventionally use a picosecond pulsed light source and a fast detector (e.g., digitizers/oscilloscopes, streak cameras, and others). These properties are determined based on their expected effect on the time-resolved signal. For instance, higher sample absorption results in a quicker decay of the detected signal over time, as the attenuation is higher as light travels within the sample for larger times (chapter 5, section 5.2 Absorption processes). Time-resolved measurements are the most suitable for accurate measurements of tissue absorption and scattering properties due to the independence between effects of light propagation of signals related to absorption (temporal pulse narrowing; section 5.2 Absorption processes) and scattering (temporal pulse broadening and shift towards longer times section 5.1 Elastic and inelastic scattering processes). Still, it is important to note that time-resolved measurements typically require detection of sufficient numbers of photons without increasing illumination intensity above the threshold which can bias photon counting. This requirement makes the development of fast electronics and fast/ultrafast lasers one of the bottlenecks to advance the study of biological media, especially if portable and transportable systems stable at flexible surrounding environment conditions (vibrations, temperature, humidity, electric stability, local electromagnetic fields, etc) have to be developed.

The accuracy on the determination of sample absorption and scattering properties as well as fluorescence/phosphorescence lifetimes is dependent on:

- **Illumination pulse width:** the pulse width together with the broadening caused by other system components (instrument response function) determines the minimum signal width that can be obtained in response to light propagation in the sample. The pulse width of the light source should be chosen so that the broadening or expected fluorescence/phosphorescence decays fall within the measurement time window, while the minimum width should still be within the time resolution of the detector. Time-resolved techniques commonly use laser sources to generate pulses of tens-to-hundred of picoseconds.
- **Instrument response function (IRF):** once the light pulse travels through all the system components and reaches the detector, this pulse is broadened by diverging optical paths within the system due to optical aberrations, and differences in position of light rays, angles it reaches optical components with varying refractive indexes, reflection properties etc. The actual pulse width is typically detected with a delay due to the system electronics, which may contribute to the pulse broadening. Optical and electronic broadening of the illumination pulse makes every signal to be detected with after its convolution with an instrument response function (chapter 5 section 5.5 Implications on modeling light behavior in reflectance and transmittance geometries). For instance, the detected signal from a laser pulse is the convolution between this pulse and the IRF. The same is valid for light which traveled through the sample. Even though pulses are expected to be narrower upon propagation throughout absorbing media, they are not expected to be narrower than the IRF. If signals are expected to be collected from highly scattering media or long fluorescence/phosphorescence lifetimes, the IRF should be narrow enough so that most part of the

detected signals (convolution between sample signal and IRF, e.g., broadened IRF due to scattering, or a fluorescence decay) are still within the measurement time window.

- **Measurement time window (also known as signal period):** measurement/acquisition time is the duration of time in which data is collected and recorded. Although data can be detected in multiple ways, the detector is not necessarily always collecting photons, and capturing sample signals higher than noise typically require recording for sufficiently long periods of time (long integration times of a few seconds), as source power is usually low (µW to mW) due to laser safety requirements for tissue measurements or not to heat biofluid/biosolid samples. Also, detected light intensities (photon count rates) cannot be high to not saturate detector or not to cause the pile-up effect (discussed below in Temporal stability of collected signal). Therefore, signals need to be collected in response to a period sequence of light pulses, which will limit the time window available for photon collection/recording after every pulse. The period of pulses and detector recovery time (i.e., the time required for the detector to be available for the next measurement – also known as detector deadtime) determine the measurement time window and the effective photon counting time of the optical system.
- **Stability of signal amplitude (light source intensity fluctuations, electronic noise, and detector after-pulsing):** error on time-resolved signals can arise from unpredictable (not possible to correct for) amplitude fluctuations resulting from light intensity variations, changes on detector sensitivity, electronic noise, and the after-pulsing effect. Instrumental errors can have many sources including factors of the surrounding environment such as local vibrations, temperature or electrical stability of local facilities (which can change electronic responses of the optical systems and even cause small displacement of optical components if these components are miniaturized and the system requires high alignment accuracy). Still, after-pulsing may remain unpredictable, as it comprises of the generation of a pseudo-signal (afterpulse) after each real signal pulse due to the release of trapped charge carriers at random times in detectors based on the avalanche process of detection (i.e., electron multiplication for generation of detectable current, in very simple words). Avalanche processes can be initiated in the absence of intrinsic dark carriers or photo-generated carriers.
- **Temporal stability of generated and detected signals (timing jitter and phase noise):** accurate determination of optical properties from measured signals relies on their high temporal stability, which is associated with the narrowest IRF that could be measured with an optical system. For instance, the IRF width determines the highest absorption coefficient which can be estimated by a time-of-flight system, or the shortest fluorescence lifetime which can be measured by a time-resolved fluorescence spectroscopy system. The temporal stability of a time-resolved detector is primarily dependent on the detector, source and electronics. In general, light pulses can be generated by the light source in slightly different times at every period. The measurement reproducibility (e.g., measurements over one day of experiment) and repeatability (e.g., measurements over one month of experiments) can provide the time fluctuation of light pulse generation. This time fluctuation is called timing jitter, and can be quantified by the deviation from expected periodicity of periodic signals such as light pulses. Most of the timing jitter comes from the detector due to the time electrons take to exit the detector depending on whether an electron-hole pair has been generated. Timing jitter is also affected by the light source, which has a delay between sending the (electronic) triggering pulse and obtaining the light pulse out. In lasers, this delay is a result of the arbitrary position in the volume where light is generated (e.g., gain medium positions within the laser cavity) and its exiting angle. The third source of timing jitter is the system electronics, which can have multiple sources of timing fluctuations including period jitter, edge or phase jitter (i.e., the time interval error), and cycle-to-cycle jitter (i.e., the difference between the periods of adjacent cycles). Timing jitter can be corrected when the source signal is recorded together with sample signals and/or when the intensity rise of sample signal is recorded with high temporal stability. However, timing jitter causes significant errors for signals recorded with time-gating (sections 6.2 Time-gating and 6.4 Photon Hitting Density (PHD)), as photon detection occurs only at specific times. In time-gating, the signal cannot be corrected unless temporal corrections based on source signals are available. Finally, the temporal stability of a system can be affected by the phase noise, which is the variation in signal phase or frequency typically measured in frequency domain by evaluating the width of the signal power adjacent to the

clock fundamental. Phase noise is mainly caused by electronics and can be observed directly in highly reproducible signals as a random phase shift.

- **Signal-to-noise ratio (SNR; photon count rate, detector sensitivity and dynamic range):** information on medium absorption, scattering, fluorescence and/or phosphorescence properties highly depends on fitting time-resolved signals for functions based on involved optical processes (e.g., exponential fluorescence/phosphorescence decays) or light propagation models using diffusion theory, Monte Carlo look-up tables and other approaches. The accuracy of such fitting is determined by the SNR. For instance, the probability of estimating long fluorescence/phosphorescence lifetimes or high scattering values can be compromised by the system noise, as late photons are much less likely to be detected compared to early photons (chapters 5 and 6). Noise which degrades the SNR can be categorized into photon noise, photoelectron noise, gain noise and receiver circuit noise, which following different statistics and are dependent on the type of detector (e.g., avalanche photodiodes (APDs), photomultiplier tubes, and others) and scheme of detection used (e.g., analog, or digital detection). Photon noise (also known as shot noise and Poisson noise) determines the fundamental noise limit caused by statistics of incident photon count, which follows a Poisson distribution in which the variance is equal to its expectation. Therefore, the ratio of signal to photon noise increases with the square root of the number of photons N captured (i.e., $SNR = \sqrt{N}$). Next, the photoelectron noise occurs due to the random photocarrier generation process, in which SNR is dependent on the detector quantum efficiency η (i.e., a photon produces a photoelectron-hole pair with probability η and fails to produce it with probability $1 - \eta$). Gain noise comes from the stochastic amplification process which provides internal gain in photodetectors such as APDs. In this case, SNR is dependent on the statistics of number of photoelectrons detected, the gain imparted to a photocarrier at each time slot, and, for APDs, on the carrier ionization ratio. Last, detectors can have receiver circuit noise from several components in electrical circuitry of optical receivers (e.g., transistors, resistors, etc), which include the thermal noise (also known as Nyquist noise or Johnson noise) arising from the random motion of mobile carriers in resistive electrical materials. Receiver circuit noise is dependent on the type of circuit and can be estimated for resistance-limited and amplifier-limited receivers [9]. To improve the system SNR, increasing photon count rates and using sensitive and high-dynamic-range detectors can help. However, photon count rates should not be increased to more than (typically) 1% of repetition rate of laser pulses [10] to avoid pile-up and counting loss effects.
- **Intensity and temporal bias of collected signal (pile-up effect and counting loss):** the use of detection techniques such as time correlated single photon counting (TCSPC) requires avoiding signal intensity and temporal bias due to high photon count rates. By using TCSPC, (1) single photon events are recorded at the time of arrival of the first photon, (2) one photon is counted per excitation (light source) pulse for time correlation, and (3) all photons are summed for every time interval relative to the excitation pulse to build the time-resolved signal. Since measurements are dependent on counting the arrival time of the first photon for each signal period, reliable measurements are recorded only when the probability of not detecting a second photon arising from excitation by the same laser pulse is very low. If such second photon is generated by the sample and not measured, it causes an intensity and temporal bias in collected signal. This bias is highly dependent on the relationship between the sample photon emission time (SPET) and the detector dead time (DDT) [11]. If DDT > SPET, late emission photons will be less likely to be detected and, thus, the intensity decay of the detected signal becomes biased towards faster decays. This bias is called pile-up effect. If DDT < SPET, the detector is not being effectively used to count photons, as the sample is excited by incoming light pulses and emission occurs while the detector is not active. The non-effectiveness of photon counting is called counting loss, which leads to a general decreased intensity and SNR of detected signals with no temporal bias of photon arrival times.
- **Detector temporal resolution:** the higher the detector temporal resolution, the more accurately narrow time-resolved signals are measured, as shorter time intervals to record photon arrival times enable more precise measurement of the slope of fast time-resolved intensity decays and complex decays (i.e., measurement with small values of residues after fitting a time-of-flight curve or a time-resolved fluorescence spectroscopy curve). Since fast decays are usually associated to high absorption (or long pathlengths of light propagation in absorbing

and/or scattering media) and short fluorescence/phosphorescence lifetimes, high temporal resolution may improve accuracy of determination of their associated quantities. Also, high temporal resolution may help resolving changes in slope at complex multiexponential decays in fluorescence or phosphorescence measurements, as accuracy in the determination of decay rates and lifetimes is associated with the number of points at sufficient short time intervals to detect changes in the slope of such decays.

- **Type of analysis:** as discussed in previous chapters, analysis based on the diffusion approximation will not be as accurate compared to those of Monte Carlo simulations out of the ranges of optical properties in which diffusion theory is valid. Diffusion theory models are capable of retrieving tissue optical properties with ~10% accuracy when compared to those of tissue-mimicking phantoms [12–14]. Errors of <10% over a wide range of optical properties can be obtained by using fittings based on Monte Carlo simulations [15]. With currently sophisticated equipment, time-resolved spectroscopy can retrieve scattering and absorption properties with errors <1% [16–18].

8.1.5 Frequency-domain (FD) techniques

A number of analogies can be made between the data analysis considerations of SFD techniques in relation to those of spatially-resolved techniques, and the data analysis of FD techniques in relation to those of time-resolved techniques. In a similar way SFD uses structured illumination of fixed spatial frequencies and phases, FD uses temporal amplitude-modulated illumination of specific frequencies and phases (e.g., illumination using sinusoidally amplitude-modulated beam).

Analogies go further due to the intrinsic relationship between the pathlength (space) and time of light propagation throughout the sample (chapters 5 and 6). For instance, late photons can be collected by lower spatial or temporal frequencies, and detection of late photons enables probing deeper into the sample in reflectance/re-emittance measurements (chapter 6, sections 6.1.4 Larger or smaller spatial separation between light source and detector (i.e., larger or smaller source-to-detector distances; SDD), 6.4 Probed depth, 6.5.2 Diffuse reflectance, re-emittance or transmittance geometries). Other analogies include:

- Single-time demodulation or time-dependent (multi-time) demodulation are equivalent to single-pixel and multi-pixel demodulation of SFD signals, respectively. Then, single-time demodulation can be applied by analyzing sample responses to signals at the same frequency and different phases, whereas time-dependent demodulation is applied on signals recorded over a longer period of time. Opportunities and limitations of each type of demodulation and associated signal acquisition are similar (e.g., requirement of time stability: single-time measurements at different phases can lead to higher accuracy on the determination of optical properties at a specific time, but such accuracy cannot be obtained if the signal varies quicker than measurements are taken).
- Demodulation allows the extraction of signal amplitude and phase modulation, which are necessary to calculate sample optical properties associated with light absorption, scattering, fluorescence and phosphorescence (figure 8.1 frequency-domain spectroscopy). Absorption and scattering properties can be obtained phase shift and amplitude modulation versus the modulation frequency, including determination of μ_s' and μ_a absolute values [19–22],
- relative changes [23], fluorescence anisotropy [24], fluorescence lifetime [25–27], and phosphorescence lifetime [28].
- Time-resolved measurements can be analyzed via Fourier transform of the short pulse of light which propagated through the sample. In this case, analysis can be performed based on the broad spectrum of sinusoidal components with multiple frequencies [8].

It is worth noting that FD techniques is frequently used for imaging and tomographic applications, as signals can be captured with higher intensities and reasonable accuracy for temporally averaged optical properties compared to time-resolved signals. According to Enejder [29] measurements in intralipid phantoms performed by Madsen et. al. [21] showed average deviations of ~15% and ~5% for absorption coefficient and reduced scattering coefficient, respectively (phantoms

with absorption coefficient of ~0.1 cm^{-1}). Yet, it is worth noting that FD techniques are less accurate than time-resolved techniques and cannot currently be used for measurements of highly dynamic samples in which optical properties vary quicker than milliseconds (which can be achieved by time-resolved techniques). Finally, FD techniques cannot be used to measure short and fast fluorescence/phosphorescence lifetimes since their effects cannot be decoupled by demodulation calculations. This means only average lifetimes are calculated and probing signals from multiple luminophores is not possible with FD measurements.

8.1.6 Other techniques

In principle, optical measurement techniques can use detection of non-optical signals such as temperature (pulsed photothermal radiometry) and sound (photoacoustics), as well as use the variation of many light-based factors including polarization, light Doppler shifts, interference/diffraction (in time-domain or spectral-domain/Fourier-domain), and all geometrical factors discussed in chapter 6 (i.e., angular-resolved, numerical-aperture-resolved, depth-resolved, height-resolved techniques (the latter referring to taking measurements at various distances away from the sample surface), etc). Most of these techniques are not well researched to date, except optical coherence tomography (OCT), polarization-resolved/cross-polarization and Laser-Doppler flowmetry. Therefore, in the rest of this section, we briefly discuss the techniques most well-established among optical measurement techniques:

- Optical coherence tomography (OCT): one of the most commercially successful optical techniques used for retinal exams of many ophthalmologic clinics and a wide range of research applications, especially when combined with other optical techniques. OCT is an interferometric imaging technique which enables 3D optical scanning of biological media by measuring the intensity of backscattered light at each depth (in the same way ultrasonic pulse-echo imaging is obtained with sound waves). OCT is an extension of previous techniques called low (time) coherence reflectometry (also currently referred as time-domain OCT or TD-OCT) [30], or optical diffraction tomography (ODT), which uses single-scattered light and Fourier diffraction projection theorem [31,32] or standard diffraction tomographic methods [31,33] to reconstruct tomographic images slide-by-slice (upon acquisition of 2D images of every sample slice/cross-section). Low (time) coherence reflectometry or TD-OCT performs sample scanning by moving a reference mirror of a Michelson interferometer (sample located at the end of the arm in front of the source arm and perpendicular to the reference and detector arms) to probe interference originated from each backscattering site and reflective boundary within/on the sample. The coherence property of reflected/backscattered light provides information of the time-of-flight delay, which is associated to the probed depth (longitudinal location where the measurement was taken from). Due to the requirement of mechanically moving the reference mirror, TD-OCT has been restricted to ~400 A-scans per second with resolution limited to 10–15 μm and scans restricted to 6 radial-line scans which intersected at the fovea [34]. OCT speed has increased by ~500-1000 times (20,000–40,000 A-scans per second) and experienced decreased image resolution (~3–5 μm) and motion artifacts, as well as significantly improved the field-of-view after the introduction of wavelength tuning interferometry (WTI) [31,35,36], also known as spectral domain technology (SD-OCT) [34]. Higher spatial resolution and tissue probed depth upon incorporation of long-wavelength and narrow-bandwidth sources in swept-source OCT (SS-OCT), which currently remains as an expensive technology with limited clinical adoption. Other improvements have been made by spectroscopic OCT [37], polarization-sensitive OCT [38], and phase-sensitive OCT [39–41]. These improvements led to a broad range of medical applications to be explored with OCT Angiography (OCTA) [34,42].
- Laser-Doppler flowmetry: a technique which uses the power spectra of Doppler shifts (intensity as a function of frequency shift) to obtain information of particle movement within samples and calculate associated quantities such as microvascular blood perfusion of biological tissues. Power spectra of Doppler shifts contain information on the light-medium (e.g., light-tissue) interaction coefficient and its g-factor. Since Doppler shifts are proportional to sine of half the scattering angle (small for large g-factors), a large g-factor results in decreased

intensity at large frequency shifts. The two optical scattering parameters can be quantified by fitting Monte Carlo simulated laser Doppler spectra to that obtained experimentally. [29,43]

- Polarimetry (polarization-based techniques): uses the (diffuse) backscattered or transmitted linearly polarized light to extract patterns with characteristic azimuthal and radial variations depending on the scattering coefficient, the g-factor, optical rotation due to the presence of optically active (chiral) components, and other features of the medium. [29,44]
- A review on polarized light interaction with tissues is provided by Tuchin [45] elsewhere, and another on the selected applications and device design aspects regarding the optimal choice of the detection geometry (i.e., transmission or reflection), incident polarization states (i.e., linear or circular polarization), polarization detection schemes (i.e., Stokes or Mueller polarimetry) is given by Ghosh and Vitkin [46] also elsewhere.

8.2 Optical processes and related techniques

As previously mentioned, optical techniques can be used to extract quantities associated with sample properties based on photophysical processes such as absorption, elastic scattering, fluorescence, phosphorescence, and Raman scattering. Light signals of each photophysical process can be collected as a function of wavelength, time and at different locations of the sample by using the optical measurement techniques of section 8.1. At every illumination and collection geometry discussed in Chapter 6 (section 6.1 and 6.2), signals are generated upon exciting / illuminating the sample and collecting light reaching the detector position.

In a homogeneous semi-infinite medium, its cylindrical symmetry of light propagation allows us to define the excitation region through the depth where the depth-resolved fluence rate $\Phi_{ex}(z)$ has decayed to a fraction (e.g., 1/e) of the fluence rate at the illuminated surface, as well as the radial distance $\Phi_{\mathrm{ex}}(r) = \Phi_{\mathrm{ex}}(r,\theta), \theta \in [0, 2\pi]$ in which the radial fluence rate has decayed to a fraction (e.g., 1/e) of the fluence rate. Similarly, following the reciprocity principle of light propagation, the collection region can be defined by the depth the radial distance in which the fluence rate has decayed to the same fraction of the fluence rate at the position of the detector or collection fiber:

$$d_{excitation} = depth\left(\Phi_{ex}(z) = \frac{\max\left(\Phi_{\mathrm{ex}}(z)\right)}{e}\right)$$

$$r_{excitation} = radial\ distance\left(\Phi_{\mathrm{ex}}(r,\theta) = \frac{\max\left(\Phi_{\mathrm{ex}}(r,\theta)\right)}{e}\right)$$

$$d_{collection} = depth\left(\Phi_{\mathrm{em}}(z) = \frac{\max\left(\Phi_{\mathrm{em}}(z)\right)}{e}\right)$$

$$r_{collection} = radial\ distance\left(\Phi_{\mathrm{em}}(r,\theta) = \frac{\max\left(\Phi_{\mathrm{em}}(r,\theta)\right)}{e}\right)$$

where Φ_{ex} and Φ_{em} are the fluence rates of excitation and emission, respectively. $\Phi_{ex}(z)$ and $\Phi_{em}(z)$ can be calculated by:

$$\Phi_{ex}(z) = \int_0^{\infty}\int_0^{2\pi} \Phi_{\mathrm{ex}}(r,\theta,z)drd\theta$$

$$\Phi_{ex}(r,\theta) = \int_0^{\infty} \Phi_{\mathrm{ex}}(r,z)dz$$

$$\Phi_{em}(z) = \int_0^{\infty}\int_0^{2\pi} \Phi_{\mathrm{em}}(r,\theta,z)drd\theta$$

$$\Phi_{em}(r,\theta) = \int_0^{\infty} \Phi_{\mathrm{em}}(r,z)dz$$

To the best of my knowledge, currently there is no consensus on the value of such a fraction. If we take this fraction to be 1/e, one can define the interrogated volume based on the photon hitting density (PHD) discussed in section 6.5 of Chapter 6. It is worth noting that that the excitation and collection depend on the medium optical properties as well as the illumination and collection geometry. For instance, the excitation fluence rate would not decay as fast as a function

of distance if the illuminated area is large (compared to the decay of a small illuminated area). Similarly, for the same value of reduced scattering coefficient μ_s', fluence rates may not decay as quickly for absorption coefficients $\mu_a = 10\ cm^{-1}$ compared to $\mu_a = 100\ cm^{-1}$ (chapter 4).

The interrogated volume (IV) can be defined by the depth d_{IV} in which the $PHD(z)$, i.e., the PHD as a function of depth z (calculated by integrating PHD for each sample $r\theta$ or xy plane), decayed to $1/e^2$ of its maximum value. This depth should be higher than the depth of maximum $PHD(z)$. The interrogated volume also requires calculating the radial distance r_{IV} in which $PHD(r) = PHD(r,\theta), \theta \in [0, 2\pi]$ decay to $1/e^2$ of its maximum value, where r . The interrogated volume is the volume of the cylinder defined by the depth and lateral distance values:

$$Interrogated\ volume = d_{IV} * r_{IV}$$

where

$$d_{IV} = depth\left(PHD(z) = \frac{\max\left(PHD(z)\right)}{e^2}\right)$$

$$r_{IV} = radial\ distance\left(PHD(r) = \frac{\max\left(PHD(r)\right)}{e^2}\right)$$

and

$$PHD_{ex}(z) = \int_0^{\infty}\int_0^{2\pi} PHD_{\mathrm{ex}}(r,\theta,z)drd\theta$$

$$PHD_{ex}(r,\theta) = \int_0^{\infty} PHD_{\mathrm{ex}}(r,z)dz$$

Figure 8.2 illustrates the excitation and collection regions, as well as a sample interrogated volume for point measurement using a fiber optic probe. Based on signals collected by such a probe, information from several optical processes can be explored. In particular, the excitation and collection regions are shown for a diffuse reflectance measurement influence primarily by absorption and scattering processes. It is important to note that the representation of weaker optical processes such as fluorescence and Raman scattering would have a photon distribution following isotropic scattering for the collection / detection, as opposed to predominantly forward scattering observed for most biological tissues (Chapter 5). Hence, the calculation of collection region and interrogated volumes should take the isotropic scattering into account (especially if such calculations are based on fluence rate and PHD maps generated by Monte Carlo simulations, for example).

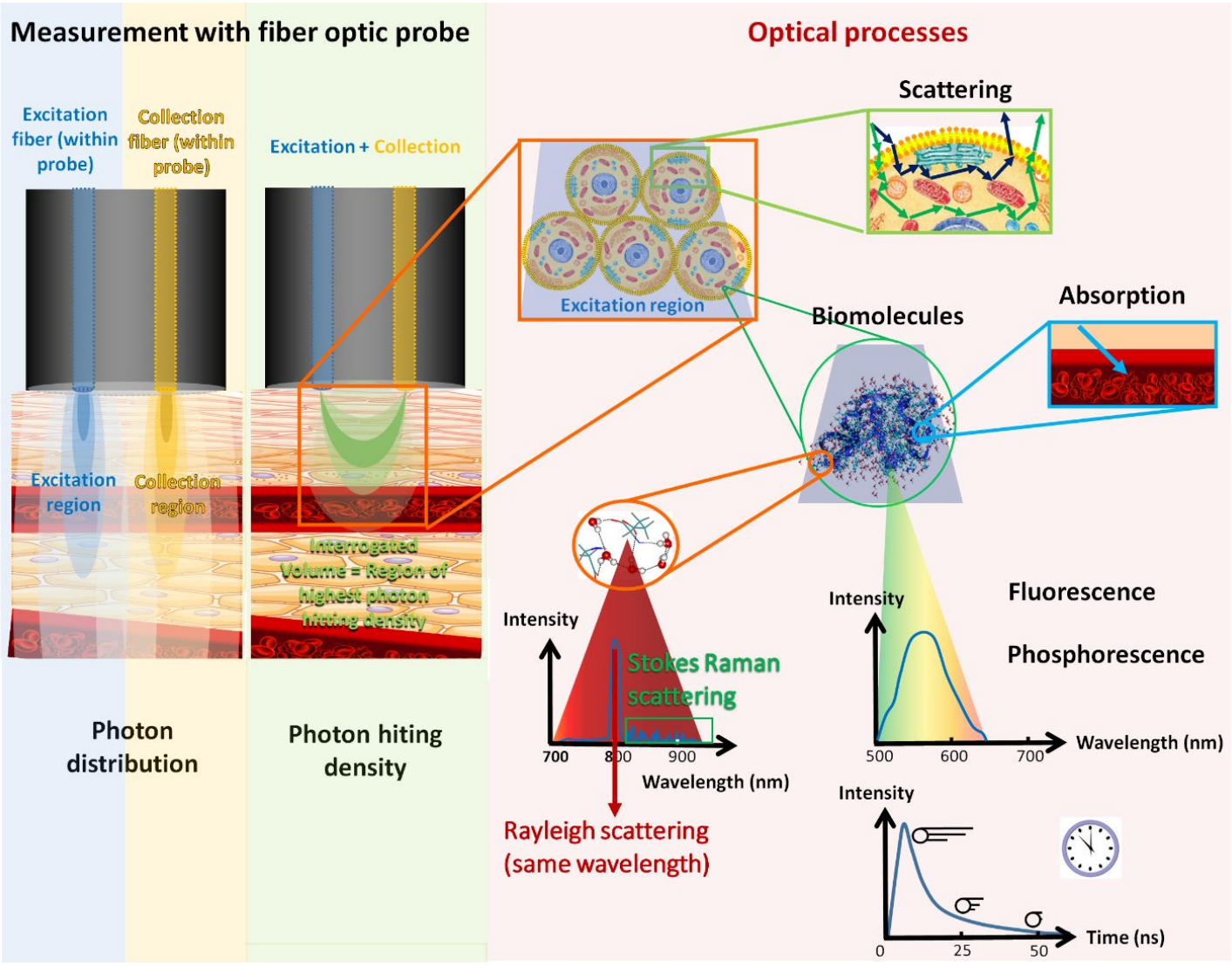


Figure 8.2: Current optical technology is based on biochemical and morphological information of biological tissues. Different information can be extracted by using optical processes such as scattering, absorption, and luminescence.

8.2.1 Diffuse reflectance spectroscopy

Diffuse reflectance spectroscopy (DRS) uses multi-chromatic light to illuminate the targeted sample/specimen/medium and is based on the analysis of its diffuse reflected light collected at micrometers to centimeters away from the illuminated spot. The diffuse reflected light consists of light which traveled inside the sample and contained information on its absorption and scattering properties. Absorption is associated with light attenuation as it propagates throughout the sample (chapter 4 and 5, sections 4.1.2 Absorption and scattering properties and 5.2 Absorption processes), whereas scattering defines how randomly light changes direction within the sample and where light exits with respect to the illuminated area (closer to such area the higher scattering the sample is; chapter 5, section 5.1 Elastic and inelastic scattering processes). Since absorption and scattering properties are related to the sample biomolecular content and microstructure, respectively, these properties are often used to differentiate samples using parameters of metabolic, functional, physiological and biological significance. In addition, information on biomolecular content and microstructure can be collected from the shallower or deeper regions within the sample by changing the probe geometry (chapter 6, sections 6.4 Probed depth and 6.5 Photon Hitting Density (PHD)) [47]. Biomolecule concentrations and scattering properties can be extracted by using inverse spectral fitting based on probabilistic or analytical models of light propagation in complex/diffuse media. This extraction enables obtaining information on parameters such as concentrations of

blood/hemoglobin, water, lipids, bile, collagen, met-hemoglobin, β-carotene, melanin, oxygen saturation (chapter 7, section 7.3 Sources of absorption in biological media), and average vessel diameter R, scattering amplitude, Mie scattering power, fraction of Rayleigh/Mie scattering and others. In biological tissues, biomolecule concentrations are determined by the electronic, vibrational and rotational energy levels of such biomolecules typically present at micromolar to nanomolar concentrations (concentrations of metabolic and immunologic markers in many types of tissue including normal and cancer tissues [48]). These concentrations can determine tissue hydration, oxygenation, and pigmentation, for instance. Scattering properties are associated with intra- and extracellular inhomogeneity of particle sizes, refractive index mismatches of several molecules and related structures (such as collagen fibrils and fibers), organelles, and cell membranes (chapter 7, section 7.1 Sources of scattering in biological media).

DRS has been used for numerous medical applications involving identification/differentiation of biological tissues and understanding molecular mechanisms behind the origin of disease. Previous DRS studies distinguished tumors from healthy surrounding tissues in breast[49,50], lung[51], and liver[52,53] and the oral cavity (head and neck cancer)[54]. Recent studies have investigated the detection of colorectal cancer during surgery with up to 100% sensitivity and specificity [55–62]. Continuous-wave (CW) DRS is suitable for diverse medical applications due to the simplicity and low cost of its instrumentation, which also enables CW-DRS instruments to be miniaturized and integrated into medical devices, portable instruments, field sensors, smartphones, smartwatches, smart-glasses, smart-socks.

DRS is a very versatile optical method with use in almost every optical measurement technique and imaging modalities. Wavelength-resolved DRS (WR-DRS) is typically used with contact point measurements for non-invasive and rapid evaluation of biochemistry and microstructure at desired tissue depths. Imaging WR-DRS is possible by combining it with spatial frequency-domain techniques. It is worth pointing out that such combination increases instrument cost and may lead to lower signal-to-noise ratios (SNR), as well as other limitations described in section 8.1.3 of this chapter, while advantages of spatial biochemical, microstructural and topographical information can be collected reasonably fast. If background is significant in targeted applications, combinations with frequency-domain techniques can help supressing background by sending and collecting signals at specific frequencies, which will be different compared to the non-modulated background signal. Finally, time-domain (TD) DRS (also known as time-of-flight (optical) spectroscopy – TOF spectroscopy - and time-domain diffuse optical spectroscopy) techniques are used for accurate measurement and decoupling of tissue absorption and scattering properties and associated determination of biomolecule concentrations and scattering-related quantities. Still, TD-DRS instrumentation is currently expensive due to the high-speed optics and electronics required, and signals are still collected with relatively low SNR compared to other techniques, which hinders the implementation of imaging TD-DRS.

Advantages of DRS from UV to near-infrared up to 2500 nm include:

- Can be used to probe non-fluorescent and non-Raman-active biomolecules, as long as they absorb light in sufficient magnitude (sufficiently high μ_a) and are present at sufficiently high concentrations to be detected.
- Strong signal in the visible and part of near-infrared wavelength ranges (currently from 400-1100 nm). Reasons:
    - Compared to other photophysical processes such as fluorescence or Raman scattering, elastically scattered light is orders of magnitude stronger.
    - most of current detectors are sensitive in the 400-1100 nm, with some of them sensitive in the UV range (typically including wavelengths from 200-900 nm) and others in the near-infrared wavelength ranges (usually from 900-1700 nm, 1100-1900 nm, 1400-2500 nm, 1000-3000 nm for commercially available spectrometers). Relatively high sensitivity can be achieved by portable spectrometers (~9 cm x 6 cm x 3 cm) in ranges between 200-850 nm.
- Lower-cost optical components (simple experimental setup required).
- Miniaturization and integration into medical devices, portable instruments, field sensors, smartphones, smartwatches, smart-glasses, smart-socks (e.g., Netflix socks), and others are facilitated by:
    - strong signal and high dynamic range of available detectors.

    - photonics integration circuits alternatives enabling reasonably powerful light sources available at diverse wavelength ranges, and moderately sensitive microdetectors.
- Wireless sensors can be enabled by lower battery requirements and longer-lasting smart sensors due to the strong signal and low signal-to-noise ratio for most systems, which decreases power requirements of light sources and detectors.
- DRS can be used for multiple micro- and macroscopic applications requiring investigation or decision-making based on the structure and biochemistry of cells, tissues, biosolids and biofluids. Reason: sensitivity to medium structure and biochemistry can be achieved by quantifying chromophore concentrations and scattering properties based on spectral fitting algorithms and multivariate analysis techniques.
- Biophotonics commercial applications range from those in environmental, food industry, pharmaceutical and cosmetic industry, agriculture, livestock, biosecurity, forensics, medical/biomedical domains, to name a few. Popular applications include (1) reflectance pulse oximetry, (2) monitoring hydration, sports performance and sleep quality (smartwatches), (3) automated identification of plant diseases via robots, (4) assessment of the quality of foods and beverages (portable and/or smartphone devices, e.g., SCIO pocket-sized NIR spectrometer and its smartphone integrated version developed in partnership with Changhong and Analog Devices [63].
- Biophotonics research applications would range from similar domains as those of commercial applications, but are extended to an even broader range of applications including (1) monitoring the treatment effectiveness of many diseases, (2) providing guidance for many types of surgical procedures, (3) identifying/diagnosing diseases, materials remaining in crime scenes, (4) performing the quality control of raw and processed materials in the manufacturing process of food, beverages, medicines, cosmetics, and others.
- In law's perspective, current commercially available DRS-based medical devices such as pulse oximeters allow a stronger motivation and quicker clinical translation of other DRS-based technologies if commercialization justifications can be made by based on the similarity of previous non-invasive devices used in clinic.

Limitations of DRS from UV to near-infrared up to 2500 nm include:

- Imaging methods may require sophisticated instrumentation.
- TD-DRS is still expensive and currently cannot be used for real-time imaging.

8.2.2 Elastic scattering spectroscopy

A subcase of DRS is elastic scattering spectroscopy (ESS), in which source and detector are close to each other (less than a few hundreds of micrometers). Similar to DRS, ESS is performed in reflectance (or re-emittance) geometry and used to extract information from scattering media, as virtually no signal would be collected for transparent media at small source-detector distances. However, typical DRS is used to collect both diffuse and subdiffuse light propagating throughout samples, whereas ESS is based on the collection of reflected subdiffuse light for applications requiring locally precise measurements of optical properties and associated parameters. Since ESS works in the subdiffuse regime (Chapter 4, sections 4.4 and 4.5), ESS signals are sensitive to sample scattering properties, and geometrical factors (such as fiber diameter and numerical aperture). Collecting primarily subdiffuse light means probing volumes close to the illuminated location such as superficial tissue or tissue close to the fiber tip. Also, subdiffuse light cannot be modeled by diffusion theory, and thus empirical models and Monte Carlo models have been developed to estimate photon path length, sampling depth, and medium optical properties [64–69].

One of the main ESS geometries is single point spectroscopy (SPS). SPS measurements can be performed by using a non-contact geometry (i.e., by illuminating and collecting light from the same pixels if using an imaging setup, or by using miniaturized light sources and detectors; Chapter 6, section 6.1.1 and 6.5.1) or a contact geometry (i.e., by using illuminating and collecting light from the same fiber, thus performing a single fiber spectroscopy). Assuming that the illuminated area is small, the main difference between non-contact and contact geometries is the collection of the light exiting at angles closer to the angle between the sample and the detector in non-contact geometry. Collecting light exiting

the sample at more specific angles is possible by increasing the distance between the detector and the sample. In non-contact and contact geometries, one can increase the specificity of collection angle by making the illuminated and detection area smaller (e.g., reducing the fiber diameter), and decreasing the numerical aperture of light sources and/or detectors. Narrowing angles can be useful in oblique measurements (Chapter 6, section 6.1.5 and 6.5.5).

It is worth noting that most scanning imaging instruments are based on SPS [70]. Also, snapshot imaging [70–72] (i.e., when detection happens while all (or most) pixels of the field of view are illuminated) is primarily based on SPS in highly scattering media, as higher scattering means more light is collected from each imaged pixel and less light will be detected from neighboring illuminated pixels, essentially increasing the resolution of determination of optical properties. In contact measurements, one of the most used SPS geometries is that of single fiber spectroscopy. In general, since non-invasive SPS imaging of superficial tissues can be offered by non-contact imaging methods, single fiber spectroscopy is used in applications requiring local detection within inhomogeneous scattering media and allowing for minimally invasive procedures for interstitial measurements. In biological tissues, single fiber spectroscopy is typically performed by using needles which are either have an optical fiber within them or consist of the optical fiber itself. Measuring within tissues means obtaining their depth-resolved optical properties, which can be used to determine the thickness of tissue layers and the distance between certain instruments (e.g., endoscope, laparoscope, cranial perforator, drill bit, etc) and the tissue relevant in a procedure (e.g., cancer tissue, brain tissue during skull bone drilling, spine within vertebrae during pedicle screw placement).

Advantages and disadvantages of ESS are similar to those of DRS, differing by only a few aspects. First, ESS imaging methods usually do not require sophisticated instrumentation. Second, in case single fiber spectroscopy is used, the procedure would not be considered non-invasive but would provide depth-resolved information at high spatial resolution. Third, ESS has stronger signal than DRS and hence light can be detected even with smaller fibers and miniaturized detectors, as well as less sensitive and cheaper detectors. Forth, since ESS works in the subdiffuse regime (Chapter 4, sections 4.4 and 4.5), detected light traveled through a much smaller pathlength within tissue and has a lower absorption and scattering probability compared with DRS. Thus, contrast to discriminate signals of samples with different optical properties is more challenging, which makes ESS suitable for sample or tissue layer differentiation based on high values of absorption coefficient (μ_a) and reduced scattering coefficient (μ_s'). This means ESS may be limited to a shorter range of wavelengths in the ultraviolet, visible, longer near-infrared or infrared wavelengths, unless the dynamic range of detectors is increased (in high scattering conditions causing the detection of primarily early photons) or the detector sensitivity increases (in high absorption and low scattering conditions limited by how much light can be detected). Fifth, ESS is only capable of superficial and local measurements within scattering media. Sixth, modeling ESS requires Monte Carlo simulations or empirical equations to correct the diffusion equation, as diffusion theory cannot be applied in subdiffusive regime conditions.

8.2.3 Infrared (IR) spectroscopy

Apart from blood and urine tests, most transmission measurements and some reflectance measurements of biological media performed with commercial instruments use infrared spectroscopy. Infrared (IR) spectroscopy is one type of vibrational spectroscopy based on the absorption of molecular vibrational modes in which vibration changes the molecular dipole moment. It is capable of identifying molecular bonds (chapter 7, section 7.3.2 Sources of mid- and far-infrared absorption in biological media) of a wide range of compounds with minimum sample volume required, reagent-free, chemical waste-free, non-invasive, non-destructive analysis. The cost-effectiveness of IR spectroscopy makes it a very attractive tool for high-throughput analysis. Efforts have been made to automate IR spectroscopy for qualitative and quantitative analysis. Yet, challenges still remain due to the strong absorption of water signal, which makes drying samples almost necessary prior to analysis and can compromise measurement reproducibility and repeatability.

IR spectroscopy can be performed in transmission, reflectance (Attenuated Total Reflection (ATR) Fourier Transform Infrared spectroscopy or ATR-FTIR spectroscopy), microscopy/imaging modes. Its reflectance mode overlaps with DRS,

and it can retrieve absorption data at wavelengths as short as those in near-infrared (NIR). However, it is worth noting that the instrumentation is fundamental limits of each technique are different, as DRS instruments are only similar to first-generation IR instruments using dispersive monochromators instead of scanned interferometry (current technology).

IR is a very mature technique, as it was created in the 19th century and first-generation IR spectrometers exist since the 1950s [73]. Still, IR spectroscopy has been dramatically improved upon implementation of fast Fourier-transform interferometry instruments in a similar way Fourier transform improved nuclear magnetic resonance (NMR) spectroscopy and mass spectrometry (MS). Improvements in IR, NMR and MS include 10^4 times more speed and 100 times higher SNR (with additional 10^4 times higher resolution and 30 times higher upper mass limits for MS) [74], which revolutionized analytical chemistry techniques available in the 1980s. Briefly, Fourier-transform infrared (FTIR) spectroscopy is performed by using Michelson interferometry to obtain the "optical path difference" spectrum (interferogram) and convert it to a wavenumber spectrum via Fourier transform. In comparison to traditional IR based on dispersive monochromators, FTIR:

- Can be made using a slit-free optical design: much higher SNR and optical throughput (Jacquinot's advantage).
- Do not require scanning using a moving grating or prism to obtain multiple wavelengths (Fellgett's advantage)
- Have higher wavenumber resolution due to typically accurate digital signal sampling coupled with a laser source. Even higher resolution can be achieved by increasing the distance/extension of mirror movement.
- Can have measurement wavenumber ranges extended (in general, towards far-IR or near-IR) by choosing appropriate light sources, beam splitters and detectors.

The short wavelength limit of FTIR is set by the wavelength of the laser used for the reference beam (typically He–Ne lasers) and the Nyquist Theorem. Considering a reference beam at 633 nm the Fourier transform does not allow accurate retrieval of periodic signals below 1400 nm without oversampling the laser. If the laser is oversampled, the wavelength of the reference beam is halved (315.5 nm) and measurements can be performed up to 700 nm.

In general, IR spectroscopy applications are based on multivariate analysis techniques for automated sample identification/differentiation, quantification of biomolecule concentration in analyzed samples. IR spectroscopy applications are separated by wavenumber ranges in a similar way the sources of IR absorption in biological media (chapter 7, section 7.3.2 Sources of mid- and far-infrared absorption in biological media). Commercially, NIR spectroscopy (12,500 – 4000 cm^{-1}) is most often used for quality control of raw/processed materials [75]. Mid-IR spectroscopy (4000-400 cm^{-1}) is typically used for biomedical applications based on the identification of carbohydrate, lipid, phospholipid, protein, amide I/II, and nucleic acid [75]. Solid-drug-molecule and excipient applications of NIR and Mid-IR spectroscopy are described more in detail by Reich [76]. Finally, far-IR spectroscopy (400-20 cm^{-1}) is typically used to study chemical and biological processes involving highly ordered structures such as protein dynamics and fibrillar formation [77] due to higher sensitivity to hydrogen bonds and peptide skeletons compared to Mid-IR [75,78]. Finally, it is worth noting that most studies of biological samples are performed primarily in the fingerprint (ranges within 1800-400 cm^{-1}) and high wavenumber (3600-2800 cm^{-1}) ranges.

Advantages of IR spectroscopy include:

- Highly-detailed IR spectra due to sharp features originated from specific IR active modes (molecular bonds whose vibration changes the molecular dipole moment).
- Highly-specific IR absorption peaks facilitate identification of associated vibrational modes and molecular bonds.
- Studies of chemical, biochemical and biological processes associated with changes in specific molecular bonds can help unveiling the molecular origin of diseases. However, one should still consider that one type of molecular bond can be found in multiple molecules and other spectroscopy techniques may be necessary to identify which specific molecules involved.
- Good SNR can be achieved by IR spectroscopy instruments since IR absorption bands are strong (large cross sections of IR transitions; chapter 4, section 4.2 Absorption).
- Fluorescence does not contaminate mid-IR and far-IR spectroscopy signals, as no fluorescence emission is generated in these wavenumber/wavelength ranges.

Still, a few disadvantages are worth point out:

- Water has a broad and strong IR absorption in terms of wavenumber/wavelength ranges, which hinders the analysis of hydrated samples.
- Building optical fiber-based instruments can be challenging due to currently toxic, fragile and/or expensive materials capable of transmitting mid-IR light [79].
- Measurement acquisition times are still long compared with other types of optical spectroscopy, which may hinder integration of IR spectroscopy into multimodal optical instruments.

8.2.4 Raman spectroscopy

Raman spectroscopy (RS) also uses a monochromatic light source to excite molecules and probe vibrational modes whose vibration alters the molecular polarizability. These vibrational modes are identified after recording the light intensity at each wavelength relatively close to the excitation wavelength, and calculating differences between the energy of the excitation light and the sample emitted light, which contain elastically scattered photons and Raman photons generated via inelastic scattering. These differences are called Raman shift. Raman spectra can be represented as a function of wavelength (nm) or Raman shifts / wavenumber (cm^{-1}) according to:

$$Wavelength\ [nm] = \lambda\ [nm] = \frac{1}{\left(\frac{1}{\lambda_{ex}[nm]} - \frac{Raman\ shift\ [cm^{-1}]}{10^7}\right)}$$

$$Raman\ shift\ [cm^{-1}]\ = \frac{1}{\left(\frac{10^7}{\lambda_{ex}[nm]} - \frac{10^7}{\lambda[nm]}\right)}$$

Raman spectra can be used to identify vibrational modes associated to molecular bonds, and potentially quantify tissue/biofluid/biosolid molecules such as carbohydrates, lipids, phospholipids, proteins, amides I/II/II, nucleic acids, and many other substances. Such identification and quantification can be made by assigning vibrational modes to Raman intensity peaks / bands (chapter 7, section 7.2 Sources of Raman scattering in biological media), which may be associated with corresponding Raman emission spectra of the pure form of particular substances. Such analysis is performed in a similar way as that of IR spectroscopy, as Raman spectra also contain specific and sharp features related to molecular vibrational modes. With this in mind, Raman is another type of vibrational spectroscopy which is complementary to IR spectroscopy. The similarity in terms of vibrational mode signals and sharp spectral features makes the analysis of RS signals very similar to that of IR spectroscopy (i.e., analysis performed by supervised and unsupervised machine learning/multivariate analysis methods, spectral fitting, peak assignments and other methods). However, applications differ, as RS systems are more expensive and RS signals are not contaminated by water absorption, which makes RS a convenient tool to analyze hydrated samples such biological cells/tissues (unlike IR spectroscopy). Since investigating biological cells/tissues is one of the primary biological applications of RS, excitation wavelengths of light sources are usually chosen between 700 and 1100 nm to ensure deeper light penetration (chapter 4, section 4.1.2 Absorption and scattering properties) and less autofluorescence (chapter 7, section 7.4 Sources of fluorescence in biological media).

The Raman spectrum is obtained by using a instrumentation focused on highly efficient wavelength selectivity to avoid signal contamination by excitation light and other sources of light within the optical system, as the objective is to collect Raman photons very unlikely to be generated (~1 Raman photon for every 10^8 excitation photons is spontaneously generated via Raman scattering [80,81], chapter 4, section 4.1.3 Inelastic scattering and luminescence). Therefore, illumination often requires lasers, which emission strongly at specific wavelengths and exhibit narrow linewidths. Once the light is shone on the sample, the emitted is collected by using lenses or optical fibers, and delivered to a detector (e.g.,

spectrometer) similarly to a fluorescence spectroscopy setup. However, in RS systems, wavelength selection is made extremely specific by using notch (i.e., narrow bandpass) filters in the illumination arm to block light of any other wavelength apart from the expected / main laser emission line (e.g., laser spontaneous emission lines and optical "noise" within the laser), as well as a dichroic beamsplitter to send red-shifted emitted light to the detector along with a long-pass filter to block backscattered light at the entrance of the detector. When using optical fibers for illumination and collection of light from samples, Raman fiber probes shoud have at least two fibers to allow illumination fiber(s) not to be used for light collection, as optical fiber materials generate substantial amounts of fluorescence and Raman photons when excited with the full laser intensity. This generation is negligible in the collection fiber, as collected photons are much fewer than excitation photons (and Raman scattering probability is low). Optimization of light collection to avoid fluorescence (isotropically emitted at all angles) can be made by surrounding a central illumination fiber with collection fibers, as Raman scattering solid angles follow those of Rayleigh scattering (strongest scattering probability forward and backwards to the direction of excitation). In this case, collection fibers should be positioned in a line at the detector end of the fiber probe to match the direction of its slit [82]. Finally, it is important to consider that RS techniques have grown to more than 25 different types to date [80] and, in this chapter, we discuss only spontaneous RS.

Advantages of RS include:

- Is not affected by water absorption, unlike IR spectroscopy.
- Easy identification and separation of sources generating Raman signals, given the sharp features of Raman spectra.
- Highly detailed and containing information of specific information of molecular bonds and related biomolecules, which may be possible to be quantified depending on the Raman emission pattern of the sample.
- Can be used to detect non-fluorescent and non-light-absorbing compounds.
- Flexible choice of excitation wavelengths, as Raman scattering can be generated at any wavelength, and of detection wavelength ranges. Preference would be given to wavelengths in which there is more Raman photons can be collected in relation to background photons (e.g., fluorescence and elastically scattered photons).

Disadvantages of RS involve:

- Weak signals due to low Raman scattering efficiencies. Weak signals compromise RS system SNR.
- Other types of light contribute to a significantly strong background, which can easily saturate RS detectors. Background is commonly generated by autofluorescence emission.
- Requires relatively intense excitation, as well as long periods of excitation and detection.
- Expensive equipment.
- RS enhanced signals may require even more expensive instrumentation, strong ultraviolet illumination (for UV resonance enhancement RS, which is not suitable for *in vivo* applications), use of potentially cytotoxic substances (e.g., nanoparticles for SERS applications) and/or increasing illumination power.

8.2.5 Fluorescence spectroscopy (FS)

Fluorescence spectroscopy (FS) uses one or combinations monochromatic light to excite specific sample molecules (fluorophores; chapter 7, section 7.4 Sources of fluorescence in biological media). When fluorophores are excited, radiative decay of fluorophores leads to fluorescence emission, whose intensity and/or decay lifetime can be recorded as fluorescence photons reach the detector (figure 1). Wavelength-dependent FS, also referred as steady-state FS (SSFS) or simply FS by most works in the current scientific literature, records the fluorescence intensity, whereas time-resolved FS (TRFS, also known as fluorescence lifetime spectroscopy; FLS) measures the temporal fluorescence decay for extraction of biomolecule-related quantities based on the fluorescence lifetime of such decay. This fluorescence lifetime corresponds

to the average amount of time a fluorophore spends in its excited state before returning to the original (ground) state. This lifetime is mostly associated to fluorophores microenvironment.

The instrumentation of FS is simple compared to other optical techniques. A monochromatic light source is chosen to excite fluorophores at their highest excitation/absorption wavelength range. If the sample consists of a mixture of fluorophores (which is usually the case for biological media), The wavelength of the light source should be at the wavelength of the highest ratio $\left(\frac{\mu_{a,targeted\ fluorophore}^{ex}}{\mu_{a,other\ fluorophores}^{ex}}\right)$ between the excitation/absorption of the targeted fluorophore ($\mu_{a,targeted\ fluorophore}^{ex}$) and that of others in such mixture ($\mu_{a,other\ fluorophores}^{ex}$). Once the light source is chosen, the main challenge is to filter out backscattered excitation light which can reach the detector (e.g., spectrometer), as dispersive elements in FS systems are usually not sufficient to avoid saturating the detector array with stray light (in spectrometers, generally consisting of light reflected of surfaces of optical components, but still sufficient to saturate the detector in many wavelengths because light arrives in diverse positions of the detector array and is usually more intense than fluorescence emission, given that excitation light is typically >100 times more intense than tissue fluorescence emission [79]). This challenge is solved via wavelength selection by using optical filters used to supress scattered/backscattered excitation light while enabling fluorescence light to be detected. These filters are usually wavelength long-pass filters or band-pass filters (also known as notch filters) in FS systems where wavelength-dependent fluorescence intensities or decays are collected.

In case fluorescence decays need to be determined for specific fluorophores, we use TRFS systems with band-pass filters at wavelength ranges of specific fluorophore emission. Even though spectrometers could be used for TRFS, currently TRFS systems are not sensitive enough to collect fluorescence emission with sufficient signal-to-noise ratio (SNR) due to detectable intensities/photon count rates limited by the speed of electronics of time-resolved detectors (section 8.1.4 Time-resolved (or time-domain) techniques). Therefore, excitation or detection can be performed by measuring fluorescence at each wavelength range at a time. This process is called wavelength multiplexing or wavelength-division multiplexing. Wavelength selection components and multiplexing excitation/emission wavelengths should maximize the collection of fluorescence emission photons of the targeted fluorophores for specific applications.

In SSFS, collecting only fluorescence emission photons means blocking excitation light while avoiding background generated by ambient light (e.g., from the sun, endoscope standard illumination, lights of surgical suites, etc) at the same wavelengths of fluorescence emission and which may be stronger than such emission. This collection is usually performed by sending/detecting illumination and collection light based on different modulated frequencies, or by time-gating illumination and collection.

Since SSFS signals are typically related to biomolecular quantities (higher fluorescence emission for larger fluorophore concentrations) and TRFS signals are most sensitive to the molecular microenvironment of fluorophores, SSFS and TRFS can be used as complementary techniques to obtain more detailed information on the sample of interest. Detailed information is generally important given the complexity of biological media. In biological tissues/cells, metabolic information can be obtained by simultaneous assessment of tissue composition and microenvironment of endogenous molecules. SSFS and TRFS can also be used with administration of exogenous contrast agents (such as indocyanine green and methylene blue) to enhance measurement sensitivity. Especially for applications involving surgical and endoscopic procedures, SSFS has been investigated as a tool to detect, diagnose and delineate margins of breast, lung, cervical, skin, oral cancers and neoplastic lesions with higher accuracy compared to white light examinations [83–92]. Similarly, TRFS has been used to differentiate tissues and study their underlying biological processes via information on biochemical composition and molecular microenvironments [93–151]. The use of TRFS has been explored to discriminate pre- and malignant lesions from normal tissues with high sensitivity and specificity [93,94,103–106,116,127,138,148–150,95,151,96–102], and has been successfully used in clinical trials [93,94,116,127,138,148–151,95–101,105].

Microscopy applications of SSFS are also widespread, especially given the control of laboratory conditions to:

- enhance background removal and increase signal-to-noise ratio

- enhance contrast through labelling/contrast agents,
- prepare samples with cells sufficiently separated from each other or organized in sufficiently few layers (up to a few hundred microns if using conventional illumination or up to a few millimetres if using nonlinear optics setups) to be imaged through microscopy systems
- monitor biochemical changes over long periods of time to study multiple biological processes,

as well as given the simplicity of SSFS optical-system implementation compared to those of other optical techniques. Eventually, research groups owning SSFS microscopy systems implemented more expensive techniques together with SSFS to study biological processes in more detail, and to explore other applications. These techniques typically include TRFS and Raman spectroscopy (RS), which can enhance molecular specificity and increase the range of molecules which can be studied using microscopy. For instance, a wide range of biomolecules and biochemical processes can be monitored using TRFS systems, including [152]:

- ionic strength
- hydrophobicity (e.g., in biopolymers)
- fluorescence quenching by oxygen (e.g., in organic complexes of ruthenium, europium, platinum, and palladium)
- calcium or chloride concentration (e.g., in neuronal systems),
- pH (e.g., in molecules' protonated and deprotonated states)
- aggregation (e.g., during internalization of dyes into cells)
- local viscosity (e.g., of liquids surroundings molecular rotors)
- local refractive index (e.g., for structure information about biological cells and tissues)
- configuration and binding to macromolecules (e.g., in dyes bonded to proteins, DNA, or lipids and monitoring of protein activities by their conformational changes)
- NAD/FAD dynamics
- drug delivery or diffusion of nanoparticles
- Förster resonance energy transfer (FRET; to investigate protein interactions and configuration),
- equilibrium between several conformational states of the fluorophore
- other factors that can deplete the excited state by resonance energy transfer.

Other effects exploited with SSFS and TRFS include [152]:

- internal quenching: internal rotation of the parts of the molecule may lead to photoisomerization, and restriction of the rotation by placement of the fluorophores into a rigid environment or lowering the temperature tends to marginalize the role of the non-radiative pathway and to increase the fluorescence and fluorescence lifetime. [152–154]
- external quenching: FRET at organic dyes, fluorescent proteins, lanthanides, quantum dots, fullerenes, carbon nanotubes and their combinations, dexter electron transfer and dynamic quenching when molecules decrease their fluorescence lifetime as a result of multiple processes at the moment of collision such as the formation of metastable complexes, resonance energy transfer, electron transfer), photon reabsorption, and excimer generation (excited dimer formation when an excited molecule associates with the same molecule in the ground state). [152–154]

Advantages of FS techniques comprise of:

- Enables investigation of multiple biological processes associated with sample biochemical composition and fluorophores (molecular) microenvironment
- Complementary molecular information can be obtained by targeting the same photophysical process with SSFS and TRFS, which enables collecting detailed information of the same molecules (fluorophores) in both techniques. This complementarity is different from that found between Raman and infrared spectroscopies, in which detailed

molecular-bond-specific information may come from different molecules (e.g., different types of protein) even when the type of molecule is the same (protein)

- Sample chemical/biochemical information can be based on multiple fluorescence-related photophysical phenomena (e.g., fluorescence decay, wavelength-dependent emission, changes induced by local viscosity, aggregation, etc) and photochemical (e.g., quenching induced by photoisomerization, proximity between functional groups, etc)
- Relatively simple optical instrumentation
- Cost-effective optical systems (multiple examples of commercial clinical systems not restricted to research purposes)
- Large SNR for imaging applications in dark-background environments
- Relatively strong signal when using exogenous fluorophores (fluorescence contrast agents) allows imaging of sample surfaces with large field-of-view
- Diverse choices of exogenous fluorophores to enhance measurement sensitivity (chapter 7, section 7.4 Sources of fluorescence in biological media)
- Exogenous fluorophores with high quantum yield (or quantum efficiency; chapter 4, section 4.1.3 Inelastic scattering and luminescence) and large excitation cross-sections [79].
- Fluorescence emission can be detected even in the presence of strong absorbers. For instance, tissue autofluorescence can be detected even at wavelength ranges where hemoglobin absorbs most light, which can be useful in clinical applications in which the signal is highly contaminated by blood absorption (as long as the fluorescence signal can be corrected by, for instance, the DRS signal in multimodal optical techniques).

Limitations of FS techniques consist of:

- Fluorescence emission of endogenous fluorophores is weak
- Multiple photophysical and photochemical processes can affect fluorescence intensity and temporal decays and add multiple confounding factors for changes in FS signals. If confounding factors are not clear, it may be difficult to identify whether biochemical alterations are associated with the target of the application in question (e.g., assessing patient disease status or identifying cancer margins), given that changes may come from sources such as specific patients instead of a disease (change in the patient status).

Take home messages

- Given the knowledge of factors affecting light propagation and distribution from previous chapters, Chapter 8 introduces ways of measuring optical signals (optical techniques) for extraction of structural and biochemical information of biological media and/or to build machine learning models by using data analysis methods of Chapters 9 and 10. The choice of optical techniques depends on their advantages and disadvantages to meet application-specific requirements [152,155–244], which is explained in subsequent Chapters of this thesis.
- Papers 1-4 [156,189,224] are based on wavelength-resolved and spatially-resolved DRS. Wavelength-resolved DRS is a mature and cost-effective technique which has been evaluated for applications in colorectal cancer detection/delineation and monitoring organ function to evaluate the possibility of clinical translation of DRS as a technique with the highest potential to be miniaturized and integrated into medical devices, given its relatively simple (and lower-cost compared to other techniques) optical setup, strong signal acquired and high dynamic range of available detectors. Drawbacks may include costs associated with instrument-based background removal (e.g., ambient light removal via modulated signals at fixed frequencies), and data exchange depending on the volume of data, type of data analysis and application requirements (e.g., rate of wireless data exchange). Spatially-resolved DRS was explored to evaluate which probe design could be more effective for colorectal cancer applications (Papers 1-3 [189,224]) based on tissue depths probed with different. source-detector distances (SDD).

Still, it is worth noting that the data of Papers 1-3 [189,224] was collected and analyzed separately for 630-μm and 2500-μm SDD probes.

- Chapter 17 is based on wavelength-resolved SSFS at 340 nm excitation, which has been chosen as an excitation wavelength which could excite most of tissue endogenous fluorophores and potentially look for biochemical differences due to changes in concentration of all of the excited fluorophores despite the low quantum yield and/or low concentration (in tissue) of some of the excited fluorophores. Fiber-optic based wavelength-resolved SSFS with epi-collection (same fiber for excitation and collection) has been explored due to its potential for clinical translation, miniaturization and integration with medical devices with similar advantages compared with wavelength-resolved DRS. Similar to wavelength-resolved DRS, drawbacks may include costs associated with instrument-based background removal, biological safety (short tissue exposure to UV light) and data exchange.
- Chapter 18 is based on wavelength-resolved RS data at 785 nm excitation, which was used collect more Raman photons in comparison with fluorescence and Mie scattered photons, as well as to generate as little fluorescence background as possible. Also, wavelength-resolved RS has been used in preliminary studies to validate the RS system for probing biological tissues for similar applications as previously discussed in this thesis (including cancer detection/delineation, cancer screening, assessment of organ function and status, treatment monitoring and understanding the molecular origin of diseases). Wavelength-resolved RS systems include both RS point spectroscopy system and the Raman microspectroscopy system, which can be used with the same laser source and spectrometer while switching between a customized fiber-optic probe and a microscopy system described in Chapter 11.
- Chapter 19 also discusses the multispectral time-resolved fluorescence spectroscopy (ms-TRFS) and imaging system to be used for future wavelength-resolved and time-resolved measurements of biological tissues in primarily surgical and endoscopic applications, but also applied to other applications. This is a very sophisticated and currently expensive system which tends to be more affordable as fast electronics capable of picosecond-resolved measurements becomes cheaper over time. However, the ms-TRFS system has been built for fast clinical translation upon technology validation by clinicians, as it already meets most clinicians' requirements for surgical systems for application validation by clinical studies. These requirements include displaying measurement results in real-time, but not machine learning outputs (such as tissue types), as these outputs require databases to be built by clinical studies (discussed in Chapter 10). Still, the possibility of measurement co-registration with histopathology, and scanning only suspect locations by clinicians (operators) decrease the measurement collection time (typically 5 minutes for each area of the body or each specimen to be scanned) while enabling the construction of a reliable database with about 100x more measurements (hundreds of thousands) compared to contact point spectroscopy (about thousands). Clinical systems will require improved miniaturization and cost-effectiveness, which will only be possible once fast detectors capable of picosecond-resolved measurements become cheaper and ms-TRFS systems become more commonly integrated into medical (possibly surgical and endoscopic) devices.

8.3 References

[1] Wang, X. and Wolfbeis, O. S., "Optical methods for sensing and imaging oxygen: materials, spectroscopies and applications," Chem. Soc. Rev. **43**(10), 3666–3761 (2014).

[2] Krafft, C. and Popp, J., "The many facets of Raman spectroscopy for biomedical analysis," Anal. Bioanal. Chem. **407**(3), 699–717 (2015).

[3] van de Giessen, M., Angelo, J. P. and Gioux, S., "Real-time, profile-corrected single snapshot imaging of optical properties," Biomed. Opt. Express **6**(10), 4051–4062 (2015).

[4] Gioux, S., Mazhar, A., Cuccia, D. J., Durkin, A. J., Tromberg, B. J. and Frangioni, J. V., "Three-dimensional surface profile intensity correction for spatially modulated imaging," J. Biomed. Opt. **14**(3), 34045 (2009).

[5] Zhao, Y., Tabassum, S., Piracha, S., Nandhu, M. S., Viapiano, M. and Roblyer, D., "Angle correction for small animal tumor imaging with spatial frequency domain imaging (SFDI)," Biomed. Opt. Express **7**(6), 2373–2384 (2016).

[6] Nguyen, J. T., Ashitate, Y., Buchanan, I. A., Ibrahim, A. M. S., Gioux, S., Patel, P. P., Frangioni, J. V and Lee, B. T., "Bone flap perfusion assessment using near-infrared fluorescence imaging," J. Surg. Res. **178**(2), e43--e50 (2012).

[7] Gioux, S., Mazhar, A. and Cuccia, D. J., "Spatial frequency domain imaging in 2019: principles, applications, and perspectives," J. Biomed. Opt. **24**(7), 71613 (2019).

[8] Lindquist, C., Pifferi, A., Berg, R., Andersson-Engels, S. and Svanberg, S., "Reconstruction of diffuse photon-density wave interference in turbid media from time-resolved transmittance measurements," Appl. Phys. Lett. **69**(12), 1674–1676 (1996).

[9] Saleh, B. E. A. and Teich, M. C., [Fundamentals of photonics], john Wiley \& sons (2019).

[10] Poudel, C., Mela, I. and Kaminski, C. F., "High-throughput, multi-parametric, and correlative fluorescence lifetime imaging," Methods Appl. Fluoresc. **8**(2), 24005 (2020).

[11] Liu, X., Lin, D., Becker, W., Niu, J., Yu, B., Liu, L. and Qu, J., "Fast fluorescence lifetime imaging techniques: A review on challenge and development," J. Innov. Opt. Health Sci. **12**(05), 1930003 (2019).

[12] Madsen, S. J., Wilson, B. C., Patterson, M. S., Park, Y. D., Jacques, S. L. and Hefetz, Y., "Experimental tests of a simple diffusion model for the estimation of scattering and absorption coefficients of turbid media from time-resolved diffuse reflectance measurements," Appl. Opt. **31**(18), 3509–3517 (1992).

[13] Cubeddu, R., Musolino, M., Pifferi, A., Taroni, P. and Valentini, G., "Time-resolved reflectance: a systematic study for application to the optical characterization of tissues," IEEE J. Quantum Electron. **30**(10), 2421–2430 (1994).

[14] Suzuki, K., Yamashita, Y., Ohta, K. and Chance, B., "Quantitative measurement of optical parameters in the breast using time-resolved spectroscopy. Phantom and preliminary in vivo results.," Invest. Radiol. **29**(4), 410–414 (1994).

[15] Pifferi, A., Taroni, P., Valentini, G. and Andersson-Engels, S., "Real-time method for fitting time-resolved reflectance and transmittance measurements with a Monte Carlo model," Appl. Opt. **37**(13), 2774–2780 (1998).

[16] Konugolu Venkata Sekar, S., Lanka, P., Farina, A., Dalla Mora, A., Andersson-Engels, S., Taroni, P. and Pifferi, A., "Broadband time domain diffuse optical reflectance Spectroscopy: A review of systems, methods, and applications," Appl. Sci. **9**(24), 5465 (2019).

[17] Lanka, S. R. P. K., Lanka, P., Yang, L., Orive-Miguel, D., Veesa, J. D., Tagliabue, S., Sudakou, A., Samaei, S., Forcione, M., Kovacsova, Z. and others., "A multi-laboratory comparison of photon migration instruments and their performances: the BitMap exercise," Opt. Tomogr. Spectrosc. Tissue XIV **11639**, 116390F (2021).

[18] Bouchard, J.-P., Veilleux, I., Jedidi, R., Noiseux, I., Fortin, M. and Mermut, O., "Reference optical phantoms for diffuse optical spectroscopy. Part 1--Error analysis of a time resolved transmittance characterization method," Opt. Express **18**(11), 11495–11507 (2010).

[19] Patterson, M. S., Moulton, J. D., Wilson, B. C., Berndt, K. W. and Lakowicz, J. R., “Frequency-domain reflectance for the determination of the scattering and absorption properties of tissue,” Appl. Opt. **30**(31), 4474–4476 (1991).

[20] Svaasand, L. O., Tromberg, B. J., Haskell, R. C., Tsay, T.-T. and Berns, M. W., “Tissue characterization and imaging using photon density waves,” Opt. Eng. **32**(2), 258–266 (1993).

[21] Madsen, S. J., Wyss, P., Svaasand, L. O., Haskell, R. C., Tadir, Y. and Tromberg, B. J., “Determination of the optical properties of the human uterus using frequency-domain photon migration and steady-state techniques,” Phys. Med. \& Biol. **39**(8), 1191 (1994).

[22] Tromberg, B. J., Svaasand, L. O., Tsay, T.-T. and Haskell, R. C., “Properties of photon density waves in multiple-scattering media,” Appl. Opt. **32**(4), 607–616 (1993).

[23] Kohl, M., Essenpreis, M. and Cope, M., “The influence of glucose concentration upon the transport of light in tissue-simulating phantoms,” Phys. Med. \& Biol. **40**(7), 1267 (1995).

[24] Lakowicz, J. R., Cherek, H., Kuśba, J., Gryczynski, I. and Johnson, M. L., “Review of fluorescence anisotropy decay analysis by frequency-domain fluorescence spectroscopy,” J. Fluoresc. **3**(2), 103–116 (1993).

[25] Mayer, R. H., Reynolds, J. S. and Sevick-Muraca, E. M., “Measurement of the fluorescence lifetime in scattering media by frequency-domain photon migration,” Appl. Opt. **38**(22), 4930–4938 (1999).

[26] Patterson, M. S. and Pogue, B. W., “Mathematical model for time-resolved and frequency-domain fluorescence spectroscopy in biological tissues,” Appl. Opt. **33**(10), 1963–1974 (1994).

[27] Boens, N., Qin, W., Basarić, N., Hofkens, J., Ameloot, M., Pouget, J., Lefevre, J.-P., Valeur, B., Gratton, E., Vandeven, M. and others., “Fluorescence lifetime standards for time and frequency domain fluorescence spectroscopy,” Anal. Chem. **79**(5), 2137–2149 (2007).

[28] Vinogradov, S. A., Fernandez-Seara, M. A., Dupan, B. W. and Wilson, D. F., “A method for measuring oxygen distributions in tissue using frequency domain phosphorometry,” Comp. Biochem. Physiol. Part A Mol. \& Integr. Physiol. **132**(1), 147–152 (2002).

[29] Enejder, A. M. K., [Light scattering and absorption in tissue-models and measurements], Lund University (1997).

[30] Huang, D., Swanson, E. A., Lin, C. P., Schuman, J. S., Stinson, W. G., Chang, W., Hee, M. R., Flotte, T., Gregory, K., Puliafito, C. A. and others., “Optical coherence tomography,” Science (80-.). **254**(5035), 1178–1181 (1991).

[31] Fercher, A. F., Drexler, W., Hitzenberger, C. K. and Lasser, T., “Optical coherence tomography-principles and applications,” Reports Prog. Phys. **66**(2), 239 (2003).

[32] Born, M. and Wolf, E., “Principles of Optics, 7th (expanded) edition,” United Kingdom Press Synd. Univ. Cambridge **461** (1999).

[33] Li, X. D., Durduran, T., Yodh, A. G., Chance, B. and Pattanayak, D. N., “Diffraction tomography for biochemical imaging with diffuse-photon density waves,” Opt. Lett. **22**(8), 573–575 (1997).

[34] Kashani, A. H., Chen, C.-L., Gahm, J. K., Zheng, F., Richter, G. M., Rosenfeld, P. J., Shi, Y. and Wang, R. K., “Optical coherence tomography angiography: a comprehensive review of current methods and clinical applications,” Prog. Retin. Eye Res. **60**, 66–100 (2017).

[35] Chinn, S. R., Swanson, E. A. and Fujimoto, J. G., “Optical coherence tomography using a frequency-tunable optical source,” Opt. Lett. **22**(5), 340–342 (1997).

[36] Hausler, G., Lindner, M. W. and others., “‘ Coherence radar’ and" spectral radar"-new tools for dermatological diagnosis,” J. Biomed. Opt. **3**(1), 21–31 (1998).

[37] Kim, J., Brown, W., Maher, J. R., Levinson, H. and Wax, A., “Functional optical coherence tomography: principles

and progress," Phys. Med. \& Biol. **60**(10), R211 (2015).

[38] Pircher, M., Hitzenberger, C. K. and Schmidt-Erfurth, U., "Polarization sensitive optical coherence tomography in the human eye," Prog. Retin. Eye Res. **30**(6), 431–451 (2011).

[39] Schwartz, D. M., Fingler, J., Kim, D. Y., Zawadzki, R. J., Morse, L. S., Park, S. S., Fraser, S. E. and Werner, J. S., "Phase-variance optical coherence tomography: a technique for noninvasive angiography," Ophthalmology **121**(1), 180–187 (2014).

[40] Wang, R. K., Kirkpatrick, S. and Hinds, M., "Phase-sensitive optical coherence elastography for mapping tissue microstrains in real time," Appl. Phys. Lett. **90**(16), 164105 (2007).

[41] Wang, R. K., Ma, Z. and Kirkpatrick, S. J., "Tissue Doppler optical coherence elastography for real time strain rate and strain mapping of soft tissue," Appl. Phys. Lett. **89**(14), 144103 (2006).

[42] Ferrara, D., Waheed, N. K. and Duker, J. S., "Investigating the choriocapillaris and choroidal vasculature with new optical coherence tomography technologies," Prog. Retin. Eye Res. **52**, 130–155 (2016).

[43] Kienle, A., Patterson, M. S., Ott, L. and Steiner, R., "Determination of the scattering coefficient and the anisotropy factor from laser Doppler spectra of liquids including blood," Appl. Opt. **35**(19), 3404–3412 (1996).

[44] Hielscher, A. H., Mourant, J. R. and Bigio, I. J., "Influence of particle size and concentration on the diffuse backscattering of polarized light from tissue phantoms and biological cell suspensions," Appl. Opt. **36**(1), 125–135 (1997).

[45] Tuchin, V. V., "Polarized light interaction with tissues," J. Biomed. Opt. **21**(7), 71114 (2016).

[46] Ghosh, N. and Vitkin, A. I., "Tissue polarimetry: concepts, challenges, applications, and outlook," J. Biomed. Opt. **16**(11), 110801 (2011).

[47] Li, W., Liu, Y. and Qian, Z., "Determination of detection depth of optical probe in pedicle screw measurement device," Biomed. Eng. Online **13**(1), 1–11 (2014).

[48] Pogue, B. W., "Optics in the molecular imaging race," Opt. Photonics News **26**(9), 24–31 (2015).

[49] De Boer, L. L., Molenkamp, B. G., Bydlon, T. M., Hendriks, B. H. W., Wesseling, J., Sterenborg, H. and Ruers, T. J. M., "Fat/water ratios measured with diffuse reflectance spectroscopy to detect breast tumor boundaries," Breast Cancer Res. Treat. **152**(3), 509–518 (2015).

[50] Soares, J. S., Barman, I., Dingari, N. C., Volynskaya, Z., Liu, W., Klein, N., Plecha, D., Dasari, R. R. and Fitzmaurice, M., "Diagnostic power of diffuse reflectance spectroscopy for targeted detection of breast lesions with microcalcifications," Proc. Natl. Acad. Sci. **110**(2), 471–476 (2013).

[51] Spliethoff, J. W., Evers, D. J., Klomp, H. M., van Sandick, J. W., Wouters, M. W., Nachabe, R., Lucassen, G. W., Hendriks, B. H. W., Wesseling, J. and Ruers, T. J. M., "Improved identification of peripheral lung tumors by using diffuse reflectance and fluorescence spectroscopy," Lung cancer **80**(2), 165–171 (2013).

[52] Evers, D. J., Nachabe, R., Hompes, D., Van Coevorden, F., Lucassen, G. W., Hendriks, B. H. W., van Velthuysen, M.-L., Wesseling, J. and Ruers, T. J. M., "Optical sensing for tumor detection in the liver," Eur. J. Surg. Oncol. **39**(1), 68–75 (2013).

[53] Tanis, E., Evers, D. J., Spliethoff, J. W., Pully, V. V, Kuhlmann, K., van Coevorden, F., Hendriks, B. H. W., Sanders, J., Prevoo, W. and Ruers, T. J. M., "In vivo tumor identification of colorectal liver metastases with diffuse reflectance and fluorescence spectroscopy," Lasers Surg. Med. **48**(9), 820–827 (2016).

[54] De Koning, S. G. B., Baltussen, E. J. M., Karakullukcu, M. B., Dashtbozorg, B., Smit, L. A., Dirven, R., Hendriks, B. H. W., Sterenborg, H. J. C. M. and Ruers, T. J. M., "Toward complete oral cavity cancer resection using a handheld diffuse reflectance spectroscopy probe," J. Biomed. Opt. **23**(12), 121611 (2018).

[55] Baltussen, E. J. M., Snæbjörnsson, P., De Koning, S. G. B., Sterenborg, H. J. C. M., Aalbers, A. G. J., Kok, N., Beets, G. L., Hendriks, B. H. W., Kuhlmann, K. F. D. and Ruers, T. J. M., "Diffuse reflectance spectroscopy as a tool for real-time tissue assessment during colorectal cancer surgery," J. Biomed. Opt. **22**(10), 106014 (2017).

[56] Baltussen, E. J. M., Kok, E. N. D., de Koning, S. G. B., Sanders, J., Aalbers, A. G. J., Kok, N. F. M., Beets, G. L., Flohil, C. C., Bruin, S. C., Kuhlmann, K. F. D. and others., "Hyperspectral imaging for tissue classification, a way toward smart laparoscopic colorectal surgery," J. Biomed. Opt. **24**(1), 16002 (2019).

[57] Baltussen, E. J. M., de Koning, S. G., Sanders, J., Aalbers, A. G. J., Kok, N. F. M., Beets, G. L., Hendriks, B. H. W., Sterenborg, H. J. C. M., Kuhlmann, K. F. D. and Ruers, T. J. M., "Using Diffuse Reflectance Spectroscopy to Distinguish Tumor Tissue From Fibrosis in Rectal Cancer Patients as a Guide to Surgery," Lasers Surg. Med. (2019).

[58] Baltussen, E. J. M., De Koning, S. G. B., Sanders, J., Aalbers, A. G. J., Kok, N. F. M., Beets, G. L., Hendriks, B. H. W., Sterenborg, H. J. C. M., Kuhlmann, K. F. D. and Ruers, T. J. M., "Tissue diagnosis during colorectal cancer surgery using optical sensing: an in vivo study," J. Transl. Med. **17**(1), 1–10 (2019).

[59] Baltussen, E. J. M., Brouwer De Koning, S. G., Hendriks, B. H. W., Jóźwiak, K., Sterenborg, H. J. C. M. and Ruers, T. J. M., "Comparing in vivo and ex vivo fiberoptic diffuse reflectance spectroscopy in colorectal cancer," Transl. Biophotonics **1**(1–2), e201900008 (2019).

[60] Baltussen, E. J. M., Sterenborg, H. J. C. M., Ruers, T. J. M. and Dashtbozorg, B., "Optimizing algorithm development for tissue classification in colorectal cancer based on diffuse reflectance spectra," Biomed. Opt. Express **10**(12), 6096–6113 (2019).

[61] Langhout, G. C., Spliethoff, J. W., Schmitz, S. J., Aalbers, A. G. J., van Velthuysen, M.-L., Hendriks, B. H. W., Ruers, T. J. M. and Kuhlmann, K. F. D., "Differentiation of healthy and malignant tissue in colon cancer patients using optical spectroscopy: A tool for image-guided surgery," Lasers Surg. Med. **47**(7), 559–565 (2015).

[62] Langhout, G. C., Spliethoff, J. W., Aalbers, A. G. J., Verwaal, V. J., Hendriks, B. H. W., Ruers, T. J. M. and Kuhlmann, K. F. D., "Colorectal Cancer Identified Using Optical Spectroscopy," Ann. Oncol. **25**, iv206 (2014).

[63] Rateni, G., Dario, P. and Cavallo, F., "Smartphone-based food diagnostic technologies: a review," Sensors **17**(6), 1453 (2017).

[64] Kanick, S. C., Sterenborg, H. and Amelink, A., "Empirical model of the photon path length for a single fiber reflectance spectroscopy device," Opt. Express **17**(2), 860–871 (2009).

[65] Kanick, S. C., Sterenborg, H. J. C. M. and Amelink, A., "Empirical model description of photon path length for differential path length spectroscopy: combined effect of scattering and absorption," J. Biomed. Opt. **13**(6), 64042 (2008).

[66] Kanick, S. C., Robinson, D. J., Sterenborg, H. and Amelink, A., "Monte Carlo analysis of single fiber reflectance spectroscopy: photon path length and sampling depth," Phys. Med. \& Biol. **54**(22), 6991 (2009).

[67] Hoy, C. L., Gamm, U. A., Sterenborg, H. J. C. M., Robinson, D. J. and Amelink, A., "Method for rapid multidiameter single-fiber reflectance and fluorescence spectroscopy through a fiber bundle," J. Biomed. Opt. **18**(10), 107005 (2013).

[68] Gamm, U. A., Kanick, S. C., Sterenborg, H., Robinson, D. J. and Amelink, A., "Measurement of tissue scattering properties using multi-diameter single fiber reflectance spectroscopy: in silico sensitivity analysis," Biomed. Opt. Express **2**(11), 3150–3166 (2011).

[69] Kanick, S. C., Gamm, U. A., Schouten, M., Sterenborg, H., Robinson, D. J. and Amelink, A., "Measurement of the reduced scattering coefficient of turbid media using single fiber reflectance spectroscopy: fiber diameter and phase function dependence," Biomed. Opt. Express **2**(6), 1687–1702 (2011).

[70] Hagen, N. A. and Kudenov, M. W., "Review of snapshot spectral imaging technologies," Opt. Eng. **52**(9), 90901

(2013).

[71] Gao, L. and Wang, L. V., "A review of snapshot multidimensional optical imaging: measuring photon tags in parallel," Phys. Rep. **616**, 1–37 (2016).

[72] Hagen, N. A., Gao, L. S., Tkaczyk, T. S. and Kester, R. T., "Snapshot advantage: a review of the light collection improvement for parallel high-dimensional measurement systems," Opt. Eng. **51**(11), 111702 (2012).

[73] Gilbert, A. S., "Vibrational, Rotational and Raman Spectroscopy, Historical Perspective" (2017).

[74] Marshall, A. G., "Fourier transform ion cyclotron resonance mass spectrometry," Acc. Chem. Res. **18**(10), 316–322 (1985).

[75] Balan, V., Mihai, C.-T., Cojocaru, F.-D., Uritu, C.-M., Dodi, G., Botezat, D. and Gardikiotis, I., "Vibrational spectroscopy fingerprinting in medicine: from molecular to clinical practice," Materials (Basel). **12**(18), 2884 (2019).

[76] Reich, G., "Mid and near infrared spectroscopy," [Analytical Techniques in the Pharmaceutical Sciences], Springer, 61–138 (2016).

[77] Durig, J. R., "Far-IR Spectroscopy, Applications," Encycl. Spectrosc. Spectrom., 498–504 (1999).

[78] Han, Y., Ling, S., Qi, Z., Shao, Z. and Chen, X., "Application of far-infrared spectroscopy to the structural identification of protein materials," Phys. Chem. Chem. Phys. **20**(17), 11643–11648 (2018).

[79] Bigio, I. J. and Fantini, S., [Quantitative biomedical optics: theory, methods, and applications], Cambridge University Press (2016).

[80] Jones, R. R., Hooper, D. C., Zhang, L., Wolverson, D. and Valev, V. K., "Raman techniques: fundamentals and frontiers," Nanoscale Res. Lett. **14**(1), 1–34 (2019).

[81] Graves, P. and Gardiner, D., "Practical raman spectroscopy," Springer (1989).

[82] Hanlon, E. B., Manoharan, R., Koo, T., Shafer, K. E., Motz, J. T., Fitzmaurice, M., Kramer, J. R., Itzkan, I., Dasari, R. R. and Feld, M. S., "Prospects for in vivo Raman spectroscopy," Phys. Med. \& Biol. **45**(2), R1 (2000).

[83] Palmer, G. M., Zhu, C., Breslin, T. M., Xu, F., Gilchrist, K. W. and Ramanujam, N., "Comparison of multiexcitation fluorescence and diffuse reflectance spectroscopy for the diagnosis of breast cancer (March 2003)," IEEE Trans Biomed Eng **50**(11), 1233–1242 (2003).

[84] Edell, E., Lam, S., Pass, H., Miller, Y. E., Sutedja, T., Kennedy, T., Loewen, G., Keith, R. L. and Gazdar, A., "Detection and localization of intraepithelial neoplasia and invasive carcinoma using fluorescence-reflectance bronchoscopy: an international, multicenter clinical trial," J Thorac Oncol **4**(1), 49–54 (2009).

[85] Thekkek, N. and Richards-Kortum, R., "Optical imaging for cervical cancer detection: solutions for a continuing global problem," Nat Rev Cancer **8**(9), 725–731 (2008).

[86] Bigio, I. J. and Mourant, J. R., "Ultraviolet and visible spectroscopies for tissue diagnostics: fluorescence spectroscopy and elastic-scattering spectroscopy," Phys. Med. Biol. **42**(5), 803–814 (1997).

[87] Breslin, T. M., "Autofluorescence and Diffuse Reflectance Properties of Malignant and Benign Breast Tissues," Ann. Surg. Oncol. **11**(1), 65–70 (2003).

[88] Drakaki, E., Kaselouris, E., Makropoulou, M., Serafetinides, A. A., Tsenga, A., Stratigos, A. J., Katsambas, A. D. and Antoniou, C., "Laser-induced fluorescence and reflectance spectroscopy for the discrimination of basal cell carcinoma from the surrounding normal skin tissue," Ski. Pharmacol Physiol **22**(3), 158–165 (2009).

[89] Freeberg, J. A., Benedet, J. L., MacAulay, C., West, L. A. and Follen, M., "The performance of fluorescence and reflectance spectroscopy for the in vivo diagnosis of cervical neoplasia; point probe versus multispectral approaches," Gynecol Oncol **107**(1 Suppl 1), S248-55 (2007).

[90] Pavlova, I., Williams, M., El-Naggar, A., Richards-Kortum, R. and Gillenwater, A., "Understanding the biological basis of autofluorescence imaging for oral cancer detection: high-resolution fluorescence microscopy in viable tissue," Clin Cancer Res **14**(8), 2396–2404 (2008).

[91] Georgakoudi, I., Sheets, E. E., Müller, M. G., Backman, V., Crum, C. P., Badizadegan, K., Dasari, R. R. and Feld, M. S., "Trimodal spectroscopy for the detection and characterization of cervical precancers in vivo," Am. J. Obstet. Gynecol. **186**(3), 374–382 (2002).

[92] Valdes, P. A., Leblond, F., Jacobs, V. L., Wilson, B. C., Paulsen, K. D. and Roberts, D. W., "Quantitative, spectrally-resolved intraoperative fluorescence imaging," Sci Rep **2**, 798 (2012).

[93] Fatakdawala, H., Gorpas, D., Bishop, J. W., Bec, J., Ma, D., Southard, J. A., Margulies, K. B. and Marcu, L., "Fluorescence Lifetime Imaging Combined with Conventional Intravascular Ultrasound for Enhanced Assessment of Atherosclerotic Plaques: an Ex Vivo Study in Human Coronary Arteries," J Cardiovasc Transl Res **8**(4), 253–263 (2015).

[94] Marcu, L., "Fluorescence lifetime techniques in medical applications," Ann Biomed Eng **40**(2), 304–331 (2012).

[95] Pfefer, T. J., Paithankar, D. Y., Poneros, J. M., Schomacker, K. T. and Nishioka, N. S., "Temporally and spectrally resolved fluorescence spectroscopy for the detection of high grade dysplasia in Barrett's esophagus," Lasers Surg Med **32**(1), 10–16 (2003).

[96] Chen, H.-M., Chiang, C.-P., You, C., Hsiao, T.-C. and Wang, C.-Y., "Time-resolved autofluorescence spectroscopy for classifying normal and premalignant oral tissues," Lasers Surg. Med. Off. J. Am. Soc. Laser Med. Surg. **37**(1), 37–45 (2005).

[97] Yong, W. H., Butte, P. V, Pikul, B. K., Jo, J. A., Fang, Q., Papaioannou, T., Black, K. L. and Marcu, L., "Distinction of brain tissue, low grade and high grade glioma with time-resolved fluorescence spectroscopy," Front. Biosci. **11**(1), 1255 (2006).

[98] Lin, W.-C., Toms, S. A., Johnson, M., Jansen, E. D. and Mahadevan-Jansen, A., "In Vivo Brain Tumor Demarcation Using Optical Spectroscopy¶," Photochem. Photobiol. **73**(4), 396 (2001).

[99] Patalay, R., Talbot, C., Alexandrov, Y., Lenz, M. O., Kumar, S., Warren, S., Munro, I., Neil, M. A., Konig, K., French, P. M., Chu, A., Stamp, G. W. and Dunsby, C., "Multiphoton multispectral fluorescence lifetime tomography for the evaluation of basal cell carcinomas," PLoS One **7**(9), e43460 (2012).

[100] Cubeddu, R., Comelli, D., D'Andrea, C., Taroni, P. and Valentini, G., "Time-resolved fluorescence imaging in biology and medicine," J. Phys. D. Appl. Phys. **35**(9), R61–R76 (2002).

[101] Marcu, L. and Hartl, B. A., "Fluorescence Lifetime Spectroscopy and Imaging in Neurosurgery," IEEE J Sel Top Quantum Electron **18**(4), 1465–1477 (2012).

[102] Gorpas, D., Fatakdawala, H., Bec, J., Ma, D., Yankelevich, D. R., Qi, J. and Marcu, L., "Fluorescence lifetime imaging and intravascular ultrasound: co-registration study using ex vivo human coronaries," IEEE Trans Med Imaging **34**(1), 156–166 (2015).

[103] Arginelli, F., Manfredini, M., Bassoli, S., Dunsby, C., French, P., Konig, K., Magnoni, C., Ponti, G., Talbot, C. and Seidenari, S., "High resolution diagnosis of common nevi by multiphoton laser tomography and fluorescence lifetime imaging," Ski. Res Technol **19**(2), 194–204 (2013).

[104] Pande, P., Shrestha, S., Park, J., Gimenez-Conti, I., Brandon, J., Applegate, B. E. and Jo, J. A., "Automated analysis of multimodal fluorescence lifetime imaging and optical coherence tomography data for the diagnosis of oral cancer in the hamster cheek pouch model," Biomed Opt Express **7**(5), 2000–2015 (2016).

[105] Phipps, J. E., Sun, Y., Fishbein, M. C. and Marcu, L., "A fluorescence lifetime imaging classification method to investigate the collagen to lipid ratio in fibrous caps of atherosclerotic plaque," Lasers Surg Med **44**(7), 564–571

(2012).

[106] Marcu, L., Fang, Q., Jo, J. A., Papaioannou, T., Dorafshar, A., Reil, T., Qiao, J. H., Baker, J. D., Freischlag, J. A. and Fishbein, M. C., "In vivo detection of macrophages in a rabbit atherosclerotic model by time-resolved laser-induced fluorescence spectroscopy," Atherosclerosis **181**(2), 295–303 (2005).

[107] Thomas, P., Pande, P., Clubb, F., Adame, J. and Jo, J. A., "Biochemical imaging of human atherosclerotic plaques with fluorescence lifetime angioscopy," Photochem Photobiol **86**(3), 727–731 (2010).

[108] Elson, D. S., Jo, J. A. and Marcu, L., "Miniaturized side-viewing imaging probe for fluorescence lifetime imaging (FLIM): validation with fluorescence dyes, tissue structural proteins and tissue specimens," New J Phys **9**, 127 (2007).

[109] Stephens, D. N., Park, J., Sun, Y., Papaioannou, T. and Marcu, L., "Intraluminal fluorescence spectroscopy catheter with ultrasound guidance," J Biomed Opt **14**(3), 30505 (2009).

[110] Phipps, J., Sun, Y., Saroufeem, R., Hatami, N. and Marcu, L., "Fluorescence lifetime imaging microscopy for the characterization of atherosclerotic plaques," Proc SPIE Int Soc Opt Eng **7161**, 71612G (2009).

[111] Sun, Y., Park, J., Stephens, D. N., Jo, J. A., Sun, L., Cannata, J. M., Saroufeem, R. M., Shung, K. K. and Marcu, L., "Development of a dual-modal tissue diagnostic system combining time-resolved fluorescence spectroscopy and ultrasonic backscatter microscopy," Rev Sci Instrum **80**(6), 65104 (2009).

[112] Dochow, S., Ma, D., Latka, I., Bocklitz, T., Hartl, B., Bec, J., Fatakdawala, H., Marple, E., Urmey, K., Wachsmann-Hogiu, S., Schmitt, M., Marcu, L. and Popp, J., "Combined fiber probe for fluorescence lifetime and Raman spectroscopy," Anal Bioanal Chem **407**(27), 8291–8301 (2015).

[113] Phipps, J. E., Hatami, N., Galis, Z. S., Baker, J. D., Fishbein, M. C. and Marcu, L., "A fluorescence lifetime spectroscopy study of matrix metalloproteinases-2 and -9 in human atherosclerotic plaque," J Biophotonics **4**(9), 650–658 (2011).

[114] Bec, J., Ma, D. M., Yankelevich, D. R., Liu, J., Ferrier, W. T., Southard, J. and Marcu, L., "Multispectral fluorescence lifetime imaging system for intravascular diagnostics with ultrasound guidance: in vivo validation in swine arteries," J Biophotonics **7**(5), 281–285 (2014).

[115] Fatakdawala, H., Poti, S., Zhou, F., Sun, Y., Bec, J., Liu, J., Yankelevich, D. R., Tinling, S. P., Gandour-Edwards, R. F., Farwell, D. G. and Marcu, L., "Multimodal in vivo imaging of oral cancer using fluorescence lifetime, photoacoustic and ultrasound techniques," Biomed Opt Express **4**(9), 1724–1741 (2013).

[116] Marcu, L., Jo, J. A., Fang, Q., Papaioannou, T., Reil, T., Qiao, J. H., Baker, J. D., Freischlag, J. A. and Fishbein, M. C., "Detection of rupture-prone atherosclerotic plaques by time-resolved laser-induced fluorescence spectroscopy," Atherosclerosis **204**(1), 156–164 (2009).

[117] Park, J., Pande, P., Shrestha, S., Clubb, F., Applegate, B. E. and Jo, J. A., "Biochemical characterization of atherosclerotic plaques by endogenous multispectral fluorescence lifetime imaging microscopy," Atherosclerosis **220**(2), 394–401 (2012).

[118] De Giorgi, V., Massi, D., Sestini, S., Cicchi, R., Pavone, F. S. and Lotti, T., "Combined non-linear laser imaging (two-photon excitation fluorescence microscopy, fluorescence lifetime imaging microscopy, multispectral multiphoton microscopy) in cutaneous tumours: first experiences," J Eur Acad Dermatol Venereol **23**(3), 314–316 (2009).

[119] Gutierrez-Navarro, O., Campos-Delgado, D. U., Arce-Santana, E. R., Maitland, K. C., Cheng, S., Jabbour, J., Malik, B., Cuenca, R. and Jo, J. A., "Estimation of the number of fluorescent end-members for quantitative analysis of multispectral FLIM data," Opt Express **22**(10), 12255–12272 (2014).

[120] Cheng, S., Rico-Jimenez, J. J., Jabbour, J., Malik, B., Maitland, K. C., Wright, J., Cheng, Y. S. and Jo, J. A., "Flexible endoscope for continuous in vivo multispectral fluorescence lifetime imaging," Opt Lett **38**(9), 1515–1517 (2013).

[121] Jabbour, J. M., Cheng, S., Malik, B. H., Cuenca, R., Jo, J. A., Wright, J., Cheng, Y. S. and Maitland, K. C., "Fluorescence

lifetime imaging and reflectance confocal microscopy for multiscale imaging of oral precancer," J Biomed Opt **18**(4), 46012 (2013).

[122] Galletly, N. P., McGinty, J., Dunsby, C., Teixeira, F., Requejo-Isidro, J., Munro, I., Elson, D. S., Neil, M. A. A., Chu, A. C., French, P. M. W. and others., "Fluorescence lifetime imaging distinguishes basal cell carcinoma from surrounding uninvolved skin," Br. J. Dermatol. **159**(1), 152–161 (2008).

[123] Yoon, Y., Jang, W. H., Xiao, P., Kim, B., Wang, T., Li, Q., Lee, J. Y., Chung, E. and Kim, K. H., "In vivo wide-field reflectance/fluorescence imaging and polarization-sensitive optical coherence tomography of human oral cavity with a forward-viewing probe," Biomed Opt Express **6**(2), 524–535 (2015).

[124] Gutierrez-Navarro, O., Campos-Delgado, D. U., Arce-Santana, E. R. and Jo, J. A., "Quadratic blind linear unmixing: A graphical user interface for tissue characterization," Comput Methods Programs Biomed **124**, 148–160 (2016).

[125] Jo, J. A., Park, J., Pande, P., Shrestha, S., Serafino, M. J., Rico Jimenez Jde, J., Clubb, F., Walton, B., Buja, L. M., Phipps, J. E., Feldman, M. D., Adame, J. and Applegate, B. E., "Simultaneous morphological and biochemical endogenous optical imaging of atherosclerosis," Eur Hear. J Cardiovasc Imaging **16**(8), 910–918 (2015).

[126] Kumar, S., Alibhai, D., Margineanu, A., Laine, R., Kennedy, G., McGinty, J., Warren, S., Kelly, D., Alexandrov, Y., Munro, I., Talbot, C., Stuckey, D. W., Kimberly, C., Viellerobe, B., Lacombe, F., Lam, E. W., Taylor, H., Dallman, M. J., Stamp, G., et al., "FLIM FRET technology for drug discovery: automated multiwell-plate high-content analysis, multiplexed readouts and application in situ," Chemphyschem **12**(3), 609–626 (2011).

[127] Coda, S., Thompson, A. J., Kennedy, G. T., Roche, K. L., Ayaru, L., Bansi, D. S., Stamp, G. W., Thillainayagam, A. V, French, P. M. W. and Dunsby, C., "Fluorescence lifetime spectroscopy of tissue autofluorescence in normal and diseased colon measured ex vivo using a fiber-optic probe," Biomed. Opt. Express **5**(2), 515–538 (2014).

[128] De Beule, P., Owen, D. M., Manning, H. B., Talbot, C. B., Requejo-Isidro, J., Dunsby, C., McGinty, J., Benninger, R. K., Elson, D. S., Munro, I., John Lever, M., Anand, P., Neil, M. A. and French, P. M., "Rapid hyperspectral fluorescence lifetime imaging," Microsc Res Tech **70**(5), 481–484 (2007).

[129] Garcia, D. I., Lanigan, P., Webb, M., West, T. G., Requejo-Isidro, J., Auksorius, E., Dunsby, C., Neil, M., French, P. and Ferenczi, M. A., "Fluorescence lifetime imaging to detect actomyosin states in mammalian muscle sarcomeres," Biophys J **93**(6), 2091–2101 (2007).

[130] Ibanez-Garcia, D., Requejo-Isidro, J., Webb, M. R., West, T. G., French, P. and Ferenczi, M. A., "Fluorescence lifetime imaging reveals that the environment of the ATP binding site of myosin in muscle senses force," Biophys J **99**(7), 2163–2169 (2010).

[131] Seidenari, S., Arginelli, F., Bassoli, S., Cautela, J., French, P. M., Guanti, M., Guardoli, D., Konig, K., Talbot, C. and Dunsby, C., "Multiphoton laser microscopy and fluorescence lifetime imaging for the evaluation of the skin," Dermatol Res Pr. **2012**, 810749 (2012).

[132] Benati, E., Bellini, V., Borsari, S., Dunsby, C., Ferrari, C., French, P., Guanti, M., Guardoli, D., Koenig, K., Pellacani, G., Ponti, G., Schianchi, S., Talbot, C. and Seidenari, S., "Quantitative evaluation of healthy epidermis by means of multiphoton microscopy and fluorescence lifetime imaging microscopy," Ski. Res Technol **17**(3), 295–303 (2011).

[133] McGinty, J., Tahir, K. B., Laine, R., Talbot, C. B., Dunsby, C., Neil, M. A., Quintana, L., Swoger, J., Sharpe, J. and French, P. M., "Fluorescence lifetime optical projection tomography," J Biophotonics **1**(5), 390–394 (2008).

[134] Tadrous, P. J., Siegel, J., French, P. M., Shousha, S., Lalani el, N. and Stamp, G. W., "Fluorescence lifetime imaging of unstained tissues: early results in human breast cancer," J Pathol **199**(3), 309–317 (2003).

[135] Park, J., Jo, J. A., Shrestha, S., Pande, P., Wan, Q. and Applegate, B. E., "A dual-modality optical coherence tomography and fluorescence lifetime imaging microscopy system for simultaneous morphological and biochemical tissue characterization," Biomed Opt Express **1**(1), 186–200 (2010).

[136] Gutierrez-Navarro, O., Arce-Santana, E. R., Campos-Delgado, D. U., Mendez, M. O. and Jo, J. A., "A new method to estimate abundances of multiple components using multi-spectral fluorescence lifetime imaging microscopy," Conf Proc IEEE Eng Med Biol Soc **2012**, 1081–1084 (2012).

[137] Jo, J. A., Applegate, B. E., Park, J., Shrestha, S., Pande, P., Gimenez-Conti, I. B. and Brandon, J. L., "In vivo simultaneous morphological and biochemical optical imaging of oral epithelial cancer," IEEE Trans Biomed Eng **57**(10), 2596–2599 (2010).

[138] Sun, Y., Phipps, J. E., Meier, J., Hatami, N., Poirier, B., Elson, D. S., Farwell, D. G. and Marcu, L., "Endoscopic fluorescence lifetime imaging for in vivo intraoperative diagnosis of oral carcinoma," Microsc Microanal **19**(4), 791–798 (2013).

[139] Shrestha, S., Park, J., Pande, P., Applegate, B. E. and Jo, J. A., "Multimodal optical imaging for simultaneous in-vivo morphological and biochemical characterization of oral epithelial cancer," Conf Proc IEEE Eng Med Biol Soc **2010**, 1970–1973 (2010).

[140] Shrestha, S., Park, J., Pande, P., Clubb, F., Applegate, B. and Jo, J. A., "Simultaneous Anatomical and Biochemical Imaging of Biological Tissue Using a Multimodal Optical Coherence Tomography and Fluorescence Lifetime Imaging System," BSuF4 (2010).

[141] Jo, J. A., Miller, M. W. and Seibel, E. J., "Time-Resolved Fluorescence Spectroscopy of the Bile Duct for Image-Guided Cancer Diagnosis," OMC6 (2011).

[142] Sun, Y., Sun, Y., Stephens, D., Xie, H., Phipps, J., Saroufeem, R., Southard, J., Elson, D. S. and Marcu, L., "Dynamic tissue analysis using time- and wavelength-resolved fluorescence spectroscopy for atherosclerosis diagnosis," Opt Express **19**(5), 3890–3901 (2011).

[143] Siegel, J., Elson, D. S., Webb, S. E. D., Benny Lee, K. C., Vlandas, A., Gambaruto, G. L., Lévêque-Fort, S., Lever, M. J., Tadrous, P. J., Stamp, G. W. H., Wallace, A. L., Sandison, A., Watson, T. F., Alvarez, F. and French, P. M. W., "Studying biological tissue with fluorescence lifetime imaging: microscopy, endoscopy, and complex decay profiles," Appl. Opt. **42**(16), 2995 (2003).

[144] Tadrous, P. J., "Methods for imaging the structure and function of living tissues and cells: 2. Fluorescence lifetime imaging," J. Pathol. **191**(3), 229–234 (2000).

[145] Patalay, R., Talbot, C., Alexandrov, Y., Munro, I., Neil, M. A., Konig, K., French, P. M., Chu, A., Stamp, G. W. and Dunsby, C., "Quantification of cellular autofluorescence of human skin using multiphoton tomography and fluorescence lifetime imaging in two spectral detection channels," Biomed Opt Express **2**(12), 3295–3308 (2011).

[146] Cole, M. J., Siegel, J., Webb, S. E. D., Jones, R., Dowling, K., Dayel, M. J., Parsons-Karavassilis, D., French, P. M. W., Lever, M. J., Sucharov, L. O. D., Neil, M. A. A., Juskaitis, R. and Wilson, T., "Time-domain whole-field fluorescence lifetime imaging with optical sectioning," J. Microsc. **203**(3), 246–257 (2001).

[147] Elson, D., Requejo-Isidro, J., Munro, I., Reavell, F., Siegel, J., Suhling, K., Tadrous, P., Benninger, R., Lanigan, P., McGinty, J., Talbot, C., Treanor, B., Webb, S., Sandison, A., Wallace, A., Davis, D., Lever, J., Neil, M., Phillips, D., et al., "Time-domain fluorescence lifetime imaging applied to biological tissue," Photochem Photobiol Sci **3**(8), 795–801 (2004).

[148] Butte, P. V, Mamelak, A. N., Nuno, M., Bannykh, S. I., Black, K. L. and Marcu, L., "Fluorescence lifetime spectroscopy for guided therapy of brain tumors," Neuroimage **54 Suppl 1**, S125-35 (2011).

[149] Thompson, A. J., Coda, S., Sorensen, M. B., Kennedy, G., Patalay, R., Waitong-Bramming, U., De Beule, P. A., Neil, M. A., Andersson-Engels, S., Bendsoe, N., French, P. M., Svanberg, K. and Dunsby, C., "In vivo measurements of diffuse reflectance and time-resolved autofluorescence emission spectra of basal cell carcinomas," J Biophotonics **5**(3), 240–254 (2012).

[150] Seidenari, S., Arginelli, F., Dunsby, C., French, P., Konig, K., Magnoni, C., Manfredini, M., Talbot, C. and Ponti, G.,

"Multiphoton laser tomography and fluorescence lifetime imaging of basal cell carcinoma: morphologic features for non-invasive diagnostics," Exp Dermatol **21**(11), 831–836 (2012).

[151] Seidenari, S., Arginelli, F., Dunsby, C., French, P. M., Konig, K., Magnoni, C., Talbot, C. and Ponti, G., "Multiphoton laser tomography and fluorescence lifetime imaging of melanoma: morphologic features and quantitative data for sensitive and specific non-invasive diagnostics," PLoS One **8**(7), e70682 (2013).

[152] Nogueira, M. S., "Fluorescence lifetime spectroscopy for diagnosis of clinically similar skin lesions" (2016).

[153] Marcu, L., French, P. and Elson, D., [Fluorescence Lifetime Spectroscopy and Imaging], CRC Press (2014).

[154] Berezin, M. Y. and Achilefu, S., "Fluorescence Lifetime Measurements and Biological Imaging," Chem. Rev. **110**(5), 2641–2684 (2010).

[155] Leal, L. B., Nogueira, M. S., Canevari, R. A. and Carvalho, L., "Vibration spectroscopy and body biofluids: Literature review for clinical applications," Photodiagnosis Photodyn. Ther. (2018).

[156] Nogueira, M. S., Raju, M., Komolibus, K., Grygoryev, K. and Andersson-Engels, S., "Assessment of tissue biochemical and optical scattering changes due to hypothermic organ preservation: a preliminary study in mouse organs," J. Phys. D. Appl. Phys. (2021).

[157] Nogueira, M. S., Raju, M., Gunther, J., Grygoryev, K., Komolibus, K., Lu, H. and Andersson-Engels, S., "Diffuse reflectance spectroscopy for determination of optical properties and chromophore concentrations of mice internal organs in the range of 350 nm to 1860 nm," Proc. SPIE 10685 Biophotonics Photonic Solut. Better Heal. Care VI **10685**, 106853G (2018).

[158] Cosci, A., Nogueira, M. S., Prataviera, S., Takahama, A., de Souza Azevedo, R. and Kurachi, C., "Time-resolved fluorescence spectroscopy for clinical diagnosis of actinic cheilitis: erratum," Biomed. Opt. Express **9**(2), 648 (2018).

[159] Nogueira, M. S., Cosci, A., Pratavieira, S., Takahama Jr, A., Azevedo, R. S. and Kurachi, C., "Evaluation of actinic cheilitis using fluorescence lifetime spectroscopy," Proc. SPIE 9703 Opt. Biopsy XIV Towar. Real-Time Spectrosc. Imaging Diagnosis **9703**, 97031U (2016).

[160] Nogueira, M. S., Komolibus, K., Grygoryev, K., Gunther, J. E. and Andersson-Engels, S., "Fluorescence spectroscopy of mouse organs using ultraviolet excitation: towards assessment of organ viability for transplantation," Proc. SPIE 10876 Opt. Interact. with Tissue Cells XXX **10876**, 1087606 (2019).

[161] Nogueira, M. S. and Guimarães, F. E. G., "Photophysical processes on biological tissues and photodynamic therapy using steady-state and time-resolved fluorescence techniques: diagnosis applications, dosimetry and photodegradation kinetics," Livro de Resumos (2016).

[162] de Paula Campos, C., de Paula D'Almeida, C., Nogueira, M. S., Moriyama, L. T., Pratavieira, S. and Kurachi, C., "Fluorescence spectroscopy in the visible range for the assessment of UVB radiation effects in hairless mice skin," Photodiagnosis Photodyn. Ther. **20**(May), 21–27 (2017).

[163] Nogueira, M. S., D'Almeida, C. P., Pratavieira, S. and Kurachi, C., "Characterization of a fluorescence lifetime spectroscopy system for diagnostic purposes using an optic fiber probe," Livro de Resumos (2014).

[164] Pires, L., Nogueira, M. S., Moriyama, L. T. and Kurachi, C., "Fluorescence lifetime for melanoma murine detection," Tech. Summ. (2014).

[165] Silami, F. D. J., Pratavieira, S., Nogueira, M. S., Barrett, A. A., Sinhoreti, M. A. C., Geraldeli, S., Pires-de-Souza, F. de C. and others., "Quantitative image of fluorescence of ceramic and resin-cement veneers," Braz. Oral Res. **33** (2019).

[166] Nogueira, M. S., Panhóca, V. H. and Bagnato, V. S., "Fluorescence spectroscopy analysis of light-induced tooth whitening," Proc. SPIE 10876, Photonics West, 10876-45 (2019).

[167] Nogueira, M., D'Almeida, C. P., Cosci, A., Pratavieira, S., Kurachi, C. and Schimdt, P. A., "Montagem e caracterização de sistema de espectroscopia e tempo de vida de fluorescência utilizando fibra óptica," XXIV Congr. Bras. Eng. Biomédica--CBEB. Uberlandia, 2468–2471 (2014).

[168] Nicolodelli, G., Tadini, A. M., Nogueira, M. S., Pratavieira, S., Mounier, S., Huaman, J. L. C., dos Santos, C. H., Montes, C. R. and Milori, D. M. B. P., "Fluorescence lifetime evaluation of whole soils from the Amazon rainforest," Appl. Opt. **56**(24), 6936–6941 (2017).

[169] Nogueira, M. S., D'Almeida, C. P., Pratavieira, S. and Kurachi, C., "Sistema de espectroscopia e tempo de vida de fluorescência para diagnóstico clinico," Anais/Resumos (2015).

[170] Kurachi, C., Pires, L., Nogueira, M. S. and Pratavieira, S., "Lifetime fluorescence for the detection of skin lesions," Biomed. Opt. 2014(April), BS4B.3 (2014).

[171] Nogueira, M. S., Pratavieira, S., Kurachi, C. and others., "Portable fluorescence microendoscope system for smartphones and imaging processing software," Tech. Summ. (2015).

[172] da Silva, A. P., Saito Nogueira, M., Jo, J. A., Salvador Bagnato, V. and Mayumi Inada, N., "Optical Based Diagnosis and Treatment of Onychomycosis," Biomed. Opt. 2016(January), JTu3A.37 (2016).

[173] de Andrade, C. T., Nogueira, M. S., Kanick, S. C., Marra, K., Gunn, J., Andreozzi, J., Samkoe, K. S., Kurachi, C. and Pogue, B. W., "Optical spectroscopy of radiotherapy and photodynamic therapy responses in normal rat skin shows vascular breakdown products," Proc. SPIE 9694 Opt. Methods Tumor Treat. Detect. Mech. Tech. Photodyn. Ther. XXV **9694**, 969410 (2016).

[174] Ono, B. A., Nogueira, M., Pires, L., Pratavieira, S. and Kurachi, C., "Subcellular localization and photodynamic activity of Photodithazine (glucosamine salt of chlorin e6) in murine melanoma B16-F10: an in vitro and in vivo study," Proc. SPIE 10476 Opt. Methods Tumor Treat. Detect. Mech. Tech. Photodyn. Ther. XXVII **10476**(February), 44 (2018).

[175] Carvalho, L. F. C. S., Nogueira, M. S., Bhattacharjee, T., Neto, L. P. M., Daun, L., Mendes, T. O., Rajasekaran, R., Chagas, M., Martin, A. A. and Soares, L. E. S., "In vivo Raman spectroscopic characteristics of different sites of the oral mucosa in healthy volunteers," Clin. Oral Investig. **23**(7), 3021–3031 (2019).

[176] Carvalho, L. F. C. S., Nogueira, M. S., Neto, L. P. M., Bhattacharjee, T. T. and Martin, A. A., "Raman spectral post-processing for oral tissue discrimination – a step for an automatized diagnostic system," Biomed. Opt. Express **8**(11), 5218 (2017).

[177] Nogueira, M. S., Pratavieira, S., Júnior, A. T., Azevedo, R. S. and Kurachi, C., "Diagnóstico de queilite actinica por espectroscopia de tempo de vida de fluorescência," Anais/Resumos (2015).

[178] Salvio, A. G., Ramirez, D. P., Inada, N. M., Stringasci, M. D., Nogueira, M. S. and Bagnato, V. S., "Fractionated illumination in a single visit photodynamic therapy for basal cell carcinoma," B. Abstr. (2017).

[179] Salvio, A. G., Ramirez, D. P., Nogueira, M. S., Stringasci, M. D., Oliveira, E. R., Inada, N. M. and Bagnato, V. S., "Evaluation of pain and treatment effect during large area photodynamic therapy in 140 patients with widespread actinic keratosis of upper limbs," B. Abstr. (2017).

[180] Nogueira, M. S., Rosa, R. G. T., Pratavieira, S., de Paula, D. and Kurachi, C., "Assembly and characterization of a fluorescence lifetime spectroscopy system for skin lesions diagnostic," Proc. SPIE 9531 Biophotonics South Am. **9531**, 95313D (2015).

[181] Nogueira, M. S., Junior, F. F. P., Caface, R. A., Oliveira, K. T. de, Bagnato, V. S. and Guimarães, F. E. G., "Characterization of photophysical properties of curcumin for theranostics of neurodegenerative diseases," Proc. SPIE 10876, Photonics West, 10876-37 (2019).

[182] Nogueira, M. S., Bagnato, V. S. and Panhoca, V. H., "Characterization of teeth fluorescence properties due to coffee

pigmentation: towards optimization of quantitative light-induced fluorescence for tooth color assessment," Proc. SPIE 11238, Photonics West, 11238-51 (2020).

[183] Nogueira, M. S., Pinto Junior, F. F., Caface, R. A., Oliveira, K. T. de and Guimarães, F. E. G., "Optimization of curcumin formulations for fluorescence-based applications," Proc. SPIE 11238, Photonics West, 11238-50 (2020).

[184] Nogueira, M. S., Bagnato, V. S. and Panhoca, V. H., "Calculation of whiteness and yellowness indexes using colorimetric and photographic methods for tooth shade evaluation," Proc. SPIE 11238, Photonics West, 11238-52 (2020).

[185] Nogueira, M. S., Brugnera Junior, A., Bagnato, V. S., Panhóca, V. H. and Panhoca, V. H., "Evaluation of the whitening effectiveness of violet illumination alone or combined with hydrogen peroxide gel," Photobiomodulation, Photomedicine, Laser Surg. (2021).

[186] Nogueira, M. S., Cosci, A. and Kurachi, C., "Assessment of oxidative stress and metabolic rates in liver grafts using time-resolved fluorescence spectroscopy," Proc. SPIE 10685 Biophotonics Photonic Solut. Better Heal. Care VI **10685**, 106853Z (2018).

[187] Nogueira, M. S. and Kurachi, C., "Assessing the photoaging process at sun exposed and non-exposed skin using fluorescence lifetime spectroscopy," Proc. SPIE 9703 Opt. Biopsy XIV Towar. Real-Time Spectrosc. Imaging Diagnosis **9703**, 97031W (2016).

[188] Pires, L., Nogueira, M. S., Pratavieira, S., Moriyama, L. T. and Kurachi, C., "Time-resolved fluorescence lifetime for cutaneous melanoma detection," Biomed. Opt. Express **5**(9), 3080 (2014).

[189] Nogueira, M. S., Raju, M., Gunther, J., Maryam, S., Amissah, M., Lu, H., Killeen, S., O'Riordain, M. and Andersson-Engels, S., "Tissue biomolecular and microstructure profiles in optical colorectal cancer delineation," J. Phys. D. Appl. Phys. (2021).

[190] Leal, L. B., Nogueira, M. S., Mageski, J. G. A., Martini, T. P., Barauna, V. G., Dos Santos, L., e Silva, L. F. das C. and others., "Diagnosis of Systemic Diseases Using Infrared Spectroscopy: Detection of Iron Overload in Plasma—Preliminary Study," Biol. Trace Elem. Res., 1–15.

[191] Panhóca, V. H., Nogueira, M. S. and Bagnato, V. S., "Treatment of facial nerve palsies with laser and endermotherapy: a report of two cases," Laser Phys. Lett. **18**(1), 15601 (2020).

[192] Nogueira, M. S., Gunther, J. E., Komolibus, K. and Andersson-Engels, S., "User-friendly graphical user interface for simulating tissue optical properties and fluence rates: improving students learning in tissue optics," Opt. Interact. with Tissue Cells XXXI **11238**, 112380B (2020).

[193] Nogueira, M. S., Gunther, J. E., Komolibus, K., Ryan, S. M., Murray, B., Jezzini, M. A., Kennedy, D. and Andersson-Engels, S., "Method of continuous improvement of multidisciplinary programs and outreach activities," Educ. Train. Opt. Photonics, 11143_41 (2019).

[194] Nogueira, M. S., Gunther, J., Komolibus, K. and Andersson-Engels, S., "Teaching light-tissue interactions: using technology for education," Opt. Interact. with Tissue Cells XXX **10876**, 108761H (2019).

[195] Nogueira, M. S., Leal, L. B., Marcarini, W. D., Pimentel, R. L., Muller, M., Vassallo, P. F., Campos, L. C. G., Dos Santos, L., Luiz, W. B., Mill, J. G. and others., "Rapid diagnosis of COVID-19 using FT-IR ATR spectroscopy and machine learning," Sci. Rep. **11**(1), 1–13 (2021).

[196] Nogueira, M. S., Leal, L. B., Marcarini, W. D., Pimentel, R. L., Muller, M., Vassallo, P. F., Campos, L. C. G., Dos Santos, L., Luiz, W. B., Mill, J. G. and others., "Author Correction: Rapid diagnosis of COVID-19 using FT-IR ATR spectroscopy and machine learning," Sci. Rep. **11**(1), 1 (2021).

[197] Nogueira, M. S., Komolibus, K., Tobo, A. L. P., Jayet, B., Sekar, S. K. V., Sorensen, S., Tyndall, C. and Andersson-Engels, S., "Biophotonics box: educational kit for multidisciplinary outreach activities in optics and photonics,"

Educ. Train. Opt. Photonics, W4B--5 (2021).

[198] "BIOPHOTONICS BOX | Marcelo Saito Nogueira | Research Project.", <https://www.researchgate.net/project/Biophotonics-box> (2 November 2021).

[199] Bunaciu, A. A., Hoang, V. D. and Aboul-Enein, H. Y., "Applications of FT-IR spectrophotometry in cancer diagnostics," Crit. Rev. Anal. Chem. **45**(2), 156–165 (2015).

[200] Nogueira, M. S., Komolibus, K., Gunther, J. E., Sekar, S. K. V., Jayet, B., Tobo, A. L. P., Li, C. L., Maryam, S., Tyndall, C., Kennedy, D. and others., "Online learning combining virtual lectures, at-home experiments and computer simulations: a multidisciplinary teaching and learning approach," Educ. Train. Opt. Photonics, F2B--6 (2021).

[201] Saito Nogueira, M., Gunther, J. E., Jayet, B., Souza Matias, J., Tyndall, C. and Andersson-Engels, S., "Biophotonics computer app: fostering multidisciplinary distance self-paced learning with a user-friendly interface," OSA Tech. Dig., 1–2 (2021).

[202] Nogueira, M. S., Amissah, M., Maryam, S., Lynch, N., Killeen, S., O'Riordain, M. and Andersson-Engels, S., "Optimization of tissue classification for colorectal cancer detection using support vector machines and diffuse reflectance spectroscopy," Eur. Conf. Biomed. Opt., EW4A--17 (2021).

[203] Nogueira, M. S., Raju, M., Gunther, J., Maryam, S., Amissah, M., Killeen, S., O'Riordain, M. and Andersson-Engels, S., "Optical determination of superficial and deeper tissue biochemistry and microstructure for delineation and early detection of colorectal cancer," Eur. Conf. Biomed. Opt., ETu3A--1 (2021).

[204] Nogueira, M. S., Maryam, S., Amissah, M., Lynch, N., Killeen, S., O'Riordain, M. and Andersson-Engels, S., "Benefit of extending near-infrared wavelength range of diffuse reflectance spectroscopy for colorectal cancer detection using machine learning," Eur. Conf. Biomed. Opt., EW4A--16 (2021).

[205] Saito Nogueira, M., Ribeiro, V., Pires, M., Peralta, F. and others., "Biochemical Profiles of In Vivo Oral Mucosa by Using a Portable Raman Spectroscopy System," Optics **2**(3), 134–147 (2021).

[206] Nogueira, M. S., Maryam, S., Amissah, M., Lu, H., Manning, E., Killeen, S., O'Riordain, M. and Andersson-Engels, S., "Broadband diffuse reflectance spectroscopy for colorectal surgical guidance (Conference Presentation)," Opt. Interact. with Tissue Cells XXXI **11238**, 1123802 (2020).

[207] Marcelo, S. N., "Biophotonics for pandemic control: large-area infection monitoring and microbial inactivation of COVID-19," Photodiagnosis Photodyn. Ther. (2020).

[208] Nogueira, M. S., "Espectroscopia de tempo de vida de fluorescência para o diagnóstico de lesões de pele clinicamente semelhantes" (2016).

[209] Nogueira, M. S., Raju, M., Gunther, J., Maryam, S., Amissah, M., Lu, H., Killeen, S., O'Riordain, M. and Andersson-Engels, S., "Accurate colorectal cancer detection and delineation by probing superficial and deeper tissue biochemistry and microstructure using diffuse reflectance spectroscopy," Proc. SPIE 11943, Photonics West, 11943-4 (2022).

[210] Carvalho, L. F. C. S., Nogueira, M. S., Neto, L. P. M., Bhattacharjee, T. T. and Martin, A. A., "Raman spectral post-processing for oral tissue discrimination--a step for an automatized diagnostic system: erratum," Biomed. Opt. Express **9**(2), 649 (2018).

[211] Panhoca, V. H., Nogueira, M. S. and Bagnato, V. S., "Laser and vacuum therapy for treatment of facial nerve palsies," Proc. SPIE 11935, Photonics West, 11935-21 (2022).

[212] Nogueira, M. S., Bagnato, V. S. and Panhoca, V. H., "Effectiveness of whitening treatments employing violet illumination alone or combined with bleaching agents," Proc. SPIE 11942, Photonics West, 11942-6 (2022).

[213] Nogueira, M. S., Maryam, S., Amissah, M., Lynch, N., Killeen, S., Lu, H., O'Riordain, M. and Andersson-Engels, S., "Improving colorectal cancer detection by extending the near-infrared wavelength range and tissue probed depth

of diffuse reflectance spectroscopy: a support vector machine approach," Proc. SPIE 11954, Photonics West, 11954-15 (2022).

[214] Ferreira, M. C. de M. S. C., Leal, L. B., Nogueira, M. S., Castro, P. A. A., Peralta, F., Zezell, D. M. and Carvalho, L. F. C. S., "Biochemical characterization of saliva of smoking and non-smoking patients by using Fourier-transform infrared spectroscopy," Proc. SPIE 11957, Photonics West, 11957-49 (2022).

[215] Nogueira, M. S., Jayet, B., Matias, J. S., Gunther, J. E., Tyndall, C. and Andersson-Engels, S., "Biophotonics web application for computer simulations in diffuse optics: fostering multidisciplinary education and research," Proc. SPIE 11958, Photonics West, 11958-18 (2022).

[216] Nogueira, M. S., Li, C. L., Maryam, S., Tyndall, C., Donovan, S., Komolibus, K., Gunther, J. E., Sekar, S. K. V., Jayet, B., Fisher, C., Kennedy, D. and Andersson-Engels, S., "Multidisciplinary teaching and learning biophotonics: assessing the effectiveness of fully online outreach events," Proc. SPIE 11958, Photonics West, 11958-39 (2022).

[217] e Silva, L. F. das C., Nogueira, M. S. and others., "New insights of Raman spectroscopy for oral clinical applications," Analyst **143**(24), 6037–6048 (2018).

[218] Carvalho, L. F. C. S., Nogueira, M. S., Bhattacharjee, T., Neto, L. P. M., Daun, L., Mendes, T. O., Rajasekaran, R., Chagas, M., Martin, A. A. and Soares, L. E. S., "In vivo Raman spectroscopic characteristics of different sites of the oral mucosa in healthy volunteers," Clin. Oral Investig., 1–11 (2018).

[219] e Silva, L. F. das C. and de Carvalho, M. S. N., "Optical techniques for fast screening--towards prevention of the coronavirus COVID-19 outbreak," Photodiagnosis Photodyn. Ther. (2020).

[220] Nogueira, M. S., "Optical theranostics and treatment dosimetry for COVID-19 lung complications: towards increasing the survival rate of vulnerable populations," Photodiagnosis Photodyn. Ther. (2020).

[221] Carnevalli, A. C., Leal, L., Scherma, A., Morais, C., Martin, F., Bonnier, F., Baker, M., Byrne, H. J., Nogueira, M. S. and others., "Identification of diabetic patients via urine analysis by FTIR: preliminary study (Conference Presentation)," Photonic Diagnosis Treat. Infect. Inflamm. Dis. II **10863**, 108630E (2019).

[222] Nogueira, M. S., "Ultraviolet-based biophotonic technologies for control and prevention of COVID-19, SARS and related disorders," Photodiagnosis Photodyn. Ther. (2020).

[223] Nogueira, M. S., "Biophotonic telemedicine for disease diagnosis and monitoring during pandemics: overcoming COVID-19 and shaping the future of healthcare," Photodiagnosis Photodyn. Ther. (2020).

[224] Nogueira, M. S., Maryam, S., Amissah, M., Lu, H., Lynch, N., Killeen, S., O'Riordain, M. and Andersson-Engels, S., "Evaluation of wavelength ranges and tissue depth probed by diffuse reflectance spectroscopy for colorectal cancer detection," Sci. Rep. **11**(1), 1–17 (2021).

[225] Nogueira, M. S., Lacerenza, M., Sekar, S. K. V., Buttafava, M., Pifferi, A., Tosi, A., Contini, D. and Andersson-Engels, S., "Broadband extraction of tissue optical properties using a portable hybrid time-resolved continuous wave instrumentation: characterization of ex vivo organs," Clin. Transl. Biophotonics, TM2B--3 (2020).

[226] Lacerenza, M., Pacheco, A., Sekar, S. K. V., Nogueira, M. S., Buttafava, M., Tosi, A., Pifferi, A., Contini, D. and Andersson-Engels, S., "Functional monitoring of lung tissue using a hybrid hyperspectral Time-Resolved GASMAS system: a systematic study on ex vivo sample.," Opt. Tomogr. Spectrosc., SW1D--2 (2020).

[227] Nogueira, M. S., Barreto, A. L., Furukawa, M., Rovai, E. S., Bastos, A., Bertoncello, G., e Silva, L. F. das C. and others., "FTIR spectroscopy as a point of care diagnostic tool for diabetes and periodontitis: A saliva analysis approach," Photodiagnosis Photodyn. Ther. **40**, 103036 (2022).

[228] Nogueira, M. S., Brugnera Junior, A., Bagnato, V. S. and Panhóca, V. H., "Evaluation of the whitening effectiveness of violet illumination alone or combined with hydrogen peroxide gel," Photobiomodulation, Photomedicine, Laser Surg. (2021).

[229] Panhóca, V. H., Nogueira, M. S. and Bagnato, V. S., “Laser and vacuum therapy for treatment of facial nerve palsies,” Imaging, Ther. Adv. Technol. Head Neck Surg. Otolaryngol. 2022 **11935**, 39–48 (2022).

[230] Nogueira, M. S., “Biophotonics for pandemic control: large-area infection monitoring and microbial inactivation of COVID-19,” Photodiagnosis Photodyn. Ther. **31**, 101823 (2020).

[231] Carvalho, L. F. das C. e S. and Saito Nogueira, M., “Optical techniques for fast screening--towards prevention of the coronavirus COVID-19 outbreak,” Photodiagnosis Photodyn. Ther. (2020).

[232] Cosci, A., Nogueira, M. S., Pratavieira, S., Takahama, A., Azevedo, R. de S., Kurachi, C. and Kurachi, C., “Time-resolved fluorescence spectroscopy for clinical diagnosis of actinic cheilitis,” Biomed. Opt. Express **7**(10), 4210–4219 (2016).

[233] Mousavi, M., Moriyama, L. T. T., Grecco, C., Nogueira, M. S., Svanberg, K., Kurachi, C. and Andersson-Engels, S., “Photodynamic therapy dosimetry using multiexcitation multiemission wavelength: toward real-time prediction of treatment outcome,” J. Biomed. Opt. **25**(6), 63812 (2020).

[234] Ferreira, M. C. C., Monteiro, G. R., Peralta, F., Castro, P. A. A., Zezell, D., Nogueira, M. S. and Carvalho, L. F. C. S., “Assessment of bound water of saliva samples by using FT-IR spectroscopy,” Lat. Am. Opt. Photonics Conf., M4B--1 (2022).

[235] Bomfin, L. S., Kitakawa, D., Nogueira, M. S., e Silva, L. F. das C. and others., “Low Level Laser Therapy as adjuvant treatment for lower lip lesion,” Lat. Am. Opt. Photonics Conf., M2B--6 (2022).

[236] Nogueira, M. S., Matthews, R., Killeen, S., O’Riordain, M. and Andersson-Engels, S., “Colorectal cancer detection based on the extraction of scattering properties and biochemical concentrations from fluorescence spectroscopy measurements,” Clin. Transl. Biophotonics, TS2B--5 (2022).

[237] Maryam, S., Nogueira, M. S., Krishnamoorthy, S., Sekar, S. K. V., Lu, H., Gautam, R., Burke, R., Andersson-Engels, S., Riordain, R. N. and Sheahan, P., “Multi-configuration Raman spectrometer for early stage diagnosis of oral cancer,” Biomed. Vib. Spectrosc. 2022 Adv. Res. Ind. **11957**, 20–26 (2022).

[238] Maryam, S., Sekar, S. K. V., Gautam, R., Kho, K. W., Ghauri, D., Nogueira, M. S., Beffara, F., Fahy, E., Riordain, R. N., Burke, R., Sheahan, P., Feeley, L. and Andersson-Engels, S., “Portable multi-configuration clinical translational Raman system for oral cancer application,” Analyst (2022).

[239] Nogueira, M. S., Ferreira, M. C. M. S. C., Leal, L. B., Castro, P. A. A., Peralta, F., Zezell, D. M. and Carvalho, L. F. C. S., “A validation step for point of care diagnostics through saliva characterization of smoking patients by using FTIR spectroscopy,” Exp. Mol. Pathol. (2023).

[240] Coelho, M. C. M. S., Leal, L. B., Nogueira, M. S., Castro, P. A. A., Peralta, F., Zezell, D. M. and others., “Biochemical characterization of saliva of smoking and non-smoking patients by using Fourier-transform infrared spectroscopy,” Biomed. Vib. Spectrosc. 2022 Adv. Res. Ind. **11957**, 86–97 (2022).

[241] Saito Nogueira, M., Maryam, S., Amissah, M., McGuire, A., Spillane, C., Killeen, S., Andersson-Engels, S. and O’Riordain, M., “Insights into Biochemical Sources and Diffuse Reflectance Spectral Features for Colorectal Cancer Detection and Localization,” Cancers (Basel). **14**(22), 5715 (2022).

[242] Panhóca, V. H., Nogueira, M. S., Zanin, F. A. A., Brugnera, A. P., Brugnera Jr, A. and Bagnato, V. S., “Dental sensitivity and color change in patients undergoing dental bleaching with application of violet light,” Oral Health Dent. Manag. **21**(6), 1–14 (2022).

[243] de Paula, D., Campos, C., Nogueira, M. S., Pratavieira, S. and Kurachi, C., “Time-resolved and steady-state fluorescence spectroscopy for the assessment of skin photoaging process,” Proc. SPIE 9531 Biophotonics South Am. **9531**, 953146 (2015).

[244] Panhóca, V. H., Aquino Junior, A. E., Souza, V. B., Ferreira, S. A., Ferreira, L. T., Souza, K. J. O., Tamae, P. E., Saito

Nogueira, M. and Bagnato, V. S., “Effects of red and infrared laser therapy in patients with tinnitus: a double-blind, clinical, randomized controlled study combining light with ultrasound, drugs and vacuum therapy,” J. Pers. Med. (2023).